SINGAPORE INSTITUTE OF TECHNOLOGY

Singapore Institute of Technology
Human Powered Submarine

NAUTICAL KNIGHTS

MAKO II

Design Report
Date of Submission: 1 June 2025

Team Members

Kim Dong Nyeok	Madhan Natarajan Mathivanan
Bryan Teo Boon Yang	Ng Zhi Loong
Teo Ai Qing	Rifhan Bin Mohamed Salehin
Tong Ming Yang	Alfred Chanokchai Law Hwee Heng
Goh Su An Edison	Lim Wei Han
Koh Ryui Zai	Tan Jin Ye
Katherlyn	Cecilia Ng Huang SiSi

Project Advisor

Associate Professor Wang Xin

Executive Summary

This report presents the comprehensive development and preparation process of the SIT Nautical Knights' second human-powered submarine, designed and built for participation in the International Submarine Races (ISR) 2025. Our team consists of eleven engineering students who focus on the overall design and fabrication of the submarine, with an additional support from media students for marketing and team development.

Key Components and Design Strategy
The development of our submarine was segmented into four major phases:

1. Research and Planning
2. Simulation and Optimization
3. Fabrication and Integration
4. Testing and Preparation

Challenges and Solutions
Through the project, our team encountered several challenges, including:

- Resource Management
- Balancing Academic Commitments
- Technical Hurdles

Benefits and Implications
The successful development and participation in the ISR 2025 offer multiple benefits:

- Educational Impact: This project has given us practical experience in engineering design, project management, and fabrication
- Industry Collaboration: Working with partners from different industries has expanded our scope or real-world engineering challenges and solutions.
- National Representative: As the first Southeast Asian team to participate in the ISR, we proudly represent Singapore on an international platform, showcasing our country's capabilities in innovation and engineering.

List of Abbreviations

Abbreviation	Description
ATA	Atmospheres Absolute
BCA	Buoyancy Control Apparatus
CFD	Computational Fluid Dynamics
eISR	European International Submarine Race
ICS	Integrated Coating Solutions
ISR	International Submarine Race
LCD	Liquid Crystal Display
LCG	Longitudinal Centre of Gravity
LCB	Longitudinal Centre of Buoyancy
MCU	Microcontroller Unit
NACA	National Advisory Committee for Aeronautics
NDU	Naval Diving Unit
PET	Polyethylene Terephthalate (foam core)
QA-1050	Quadriaxial Fiberglass (reinforcement material)
RMP	Risk Management Plan
RPM	Revolutions Per Minute
SAC	Surface Air Consumption
SIT	Singapore Institute of Technology
SP	Singapore Polytechnic
VCG	Vertical Centre of Gravity
VCB	Vertical Centre of Buoyancy

List of Tables

List of Figures

Table of Contents

1. Introduction

This report aims to detail the journey and experience of the SIT Nautical Knights team in the design, fabrication, and testing of a human-powered submarine for the International Submarine Races (ISR). This project has been undertaken by a team of undergraduate students from the Singapore Institute of Technology (SIT), fuelled by a passion for engineering, problem solving, and innovation.

Team Formation and Motivation

The SIT Nautical Knights were formed through a rigorous selection process in September 2024. Candidates were interviewed by members of the European International Submarine Races (eISR) 2024, who assessed their mindset, technical skills, and ability to work independently.

The team's motivation to join this prestigious competition stemmed from the unique opportunities it offered - international exposure, hands-on experience with advanced engineering, and the chance to take on a complex and dynamic project. Beyond technical development, the competition also inspired members to pursue new interests and push their personal and professional boundaries.

Team Members and Roles

Name	Year of Study and Course	Position
Kim Dong Nyeok	Year 3 Naval Architecture & Marine Engineering	Captain
Bryan Teo	Year 3 Naval Architecture & Marine Engineering	Propulsion Lead
Zhi Loong	Year 3 Naval Architecture & Marine Engineering	Dive Lead
Ai Qing	Year 3 Naval Architecture & Marine Engineering	Publicity Lead
Rifhan	Year 3 Naval Architecture & Marine Engineering	Team member
Cecilia	Year 3, Digital Communications and Integrated Media	Media member
Katherlyn	Year 3, Digital Communications and Integrated Media	Media member
Madhan	Year 2 Naval Architecture & Marine Engineering	Vice-Captain
Alfred	Year 2 Computer Engineering	Controls Lead
Ming Yang	Year 2 Naval Architecture & Marine Engineering	Pilot and Safety Lead
Jin Ye	Year 2 Naval Architecture & Marine Engineering	Hull Lead
Edison	Year 1 Naval Architecture & Marine Engineering	Team member
Ryui Zai	Year 1 Naval Architecture & Marine Engineering	Team member
Wei Han	Year 1 Naval Architecture & Marine Engineering	Team member

Project Timeline

- Project Kick-off: 9th October 2024
- Beginning of Fabrication: 1st January 2025
- Testing Phase: 16th April 2025
- Shipping out Submarine: 2nd June 2025

Support and Mentorship

The project team gratefully acknowledges the invaluable mentorship and support received throughout this project. We sincerely thank SIT Deputy President Mr Bernard Nee, Engineering Cluster Director Professor Tay Chuan Beng, and Lead Professional Officer Mr Michael Pilgaard Nielsen for their encouragement and institutional support. Our most profound appreciation goes to Associate Professor Wang Xin (SIT) for his leadership, academic supervision, and critical guidance as project adviser. We also thank Mr. Julian (SIT) for his technical expertise as dive advisor and Ms. Eileen Ang (SIT) for her dedicated administrative assistance.

We acknowledge SIT for providing essential resources, advanced facilities, and a strong commitment to applied learning, which were vital to the project's development and execution. Our gratitude extends to the Singapore Maritime Foundation (SMF) for its support of maritime innovation and education, which added valuable context to our work.

Finally, we recognize the significant contributions of our industry and operational partners: Mr. Alan and Mr. Tong from Integrated Coating Solutions, Dr Chia Boon Tat, Ms Xinying, Mr. Nicholas and Mr. Wei Jian from Mencast Holdings Ltd, ME6 Edwin Goh and ME4 Rhagavan from the Republic of Singapore Navy, Mr. Alex from Fishermen Scuba Studio Pte Ltd, Mr. Kelvin from Superior Machinery Equipment Limited and Mr Ong and Mr Ang from starlight. Their expertise, insights, and collaboration were crucial to the successful completion of this project.

Budget

The table below outlines the various expenses associated with this project, totalling an amount of $124,000 SGD.

Submarine Fabrication	$15,000
Logistics and Diving	$27,000
Overseas Expenses	$23,000
In-kind Contribution from Integrated Coating Solutions	$15,000
In-kind Contribution from Mencast	$15,000
In-kind Contribution from Fisherman Scuba Studio	$26,000
Miscellaneous	$3,000
Total	$124,000

Crew Training

Under the supervision of our dive advisor Mr. Matius, the team completed 1 refresher training, 2 open water dives, followed by wet testing at designated facilities. These activities were designed to enhance the team's underwater operational readiness, situational and safety awareness, and acclimatization of operating underwater and in low visibility conditions.

The refresher training was conducted at the Raffles Marina swimming pool, which has a maximum depth of 5 metres. The main objective of the refresher training was to ensure competency in basic scuba skills and align the team's scuba practices. Through this refresher training we could ensure all team members were confident and proficient before engaging in the next stage of training. The skills reviewed included breathing underwater using an air source, mask clearing, mask recovery, regulator recovery, buoyancy control, underwater communication, sharing of air source, free flow regulator, buddy system and basic equipment setup and safety checks. These exercises were essential in building diver awareness, aligning scuba practices and reinforcing safety protocols.

The open water dives were conducted off the Southern coast of Singapore - Pulau Hantu (Ghost Island). The objective was to simulate and acclimatise to the expected conditions of the competition venue. The team dived at depths between 5 metres to 15 metres to understand how light affects visibility. These dives allowed the team to understand their limitations in low visibility conditions and devise protocols to improve their communication, coordination, and situational awareness.

Following the refresher training and open water dives, a series of wet tests was conducted at both Singapore Polytechnic's swimming pool (2.3 metres) and the Naval Diving Unit (NDU) confined pool training facility (10 metres). These controlled environments enabled the team to validate the submarine's functionality and refine operational procedures.

During wet testing, the team also performed a series of safety drills to validate the pilot's readiness and confidence. These drills included deployment of safety buoy, simulated emergency pilot egress and underwater maintenance exercises, to ensure readiness for potential issues during competition scenarios.

2. Design Philosophy

The design philosophy of MAKO II centres on the pursuit of speed, safety, and modularity. As Singapore's first entry into the International Submarine Race (ISR), our goal was not only to compete but to embody a new design benchmark for future Southeast Asian teams. The submarine was conceptualized to balance optimal hydrodynamic performance with practical fabrication and pilot comfort, an engineering solution shaped by iterative design, extensive testing, and real-world limitations.
The approach emphasizes the following principles:

- **Efficiency-Driven Development:** Using Computational Fluid Dynamics (CFD) simulations and SolidWorks parametric modelling, we iterated through over 50 design variants to minimize drag forces and reduce surface area. The final configuration achieved a 15% reduction in drag relative to MAKO I.
- **Sustainability and Modularity:** The submarine is fully modular, designed for efficient transport, storage, and repairs. Components including the drivetrain, control surfaces, and hull are independently detachable, enabling streamlined shipping and maintenance.
- **Safety-First Mindset**: Safety is embedded from the start. The dead man's switch buoy, reinforced escape hatches, pilot emergency protocols, and robust training were all engineered into the submarine with minimal compromise to performance.
- **Human-Centred Engineering:** The pilot is at the core of the design. The ergonomics of a forward-leaning, cyclist-inspired posture became the basis for all subsequent decisions, from drivetrain configuration to hull dimensions.
-

Team objectives

A vote was conducted to determine team priorities, and the outcome was categorised using the MoSCoW method. The summarized result are as follows.

Team Objectives	**Votes**
Overall Performance	✓✓✓✓✓
Most Innovative Propulsion	✓
Best Use of Technology	✓
Absolute speed	✓✓✓✓✓✓
Best Design	✓✓
Smooth Operation	✓✓✓✓✓
Best Spirit of the Races	✓✓✓✓
Fastest Speed by Category	✓✓✓✓✓✓

3. Engineering Aspects & Design Details

3.1 The Pilot

The design process began with the selection of a team member of smaller stature; this member would represent the team as the pilot. The team would create a 1:1 scale model of the pilot in SolidWorks. This provided a foundation to model the internal systems and external hull around. For the 2024 eISR, the pilot adopted a supine position, which naturally led to a streamlined hull design. This year, the team performed a Computational Fluid Dynamics (CFD) analysis on a preliminary hull and compared its performance to that of the 2024 design. The results indicated that drag force was the dominant resistance factor at our target speeds of 5 to 9 knots for both hulls. Based on our understanding, the primary contributors to drag are the hull's surface area and its frictional coefficient. Therefore, the team focused on reducing the external surface area of the submarine. This objective will be achieved through the optimization of the pilot's posture and spatial arrangement within the hull.

Table 1. Pilot Dimensions

Part	Dimension (mm)
Shoulder width	440
Sole to Knee	490
Knee to Tailbone	550
Tailbone to Shoulder	600

The pilot's chosen posture will be similar to a professional cyclist, where his waist will be the highest point, and his back will be angled slightly downwards, with his shoulder located at the centre (vertically). The pilot's legs were brought forward to enable the pilot to input the maximum power.

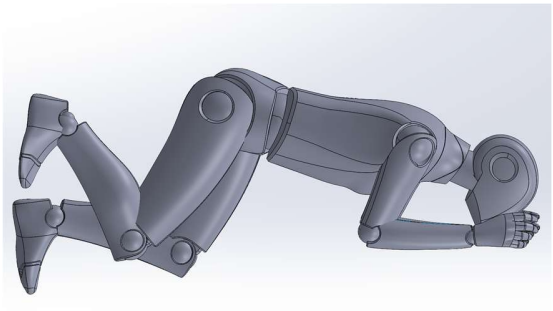

Figure 1: Model of Pilot Position

3.2 Propulsion System

This section outlines the implementation of the propulsion system, which comprises several key components, each meticulously designed and implemented to ensure performance and efficiency. In this year's ISR, the team decided to reuse a modified version of the drive train system previously utilized in MAKO I, which competed in the eISR. This decision was made to reduce the wastage and spending on new components. An overview of MAKO I and MAKO II components can be seen below.

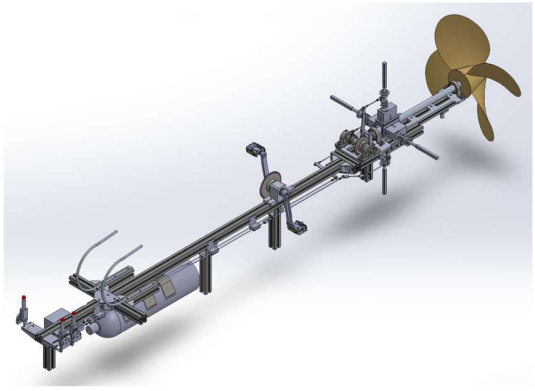

Figure 2: MAKO I Propulsion System

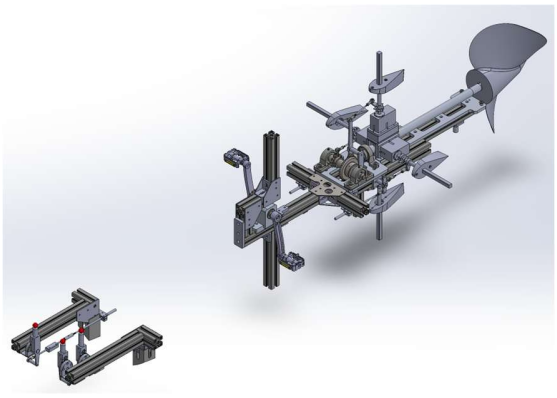

Figure 3: MAKO II Propulsion System

3.2.1 Drive train

The drivetrain from MAKO I had a longitudinal aluminium profile stretching from the bow to the stern of the submarine, which accommodated the supine position of the pilot. This allowed the pilot's controls to be transmitted via mechanical control linkages running along the longitudinal profile. To improve longevity of the drivetrain, many components that were previously made from cast iron and prone to failure were replaced with stainless steel alternatives. Leading to an increase of overall weight of the drivetrain.

Table 2. MAKO I Drivetrain Specifications

	Dimensions
Length	3234mm
Weight	30kg
Mounting points	4
Estimated Pilot Cadence	50 RPM
Sprocket Gear ratio	1:3
Bevel Gear ratio	1:2
Propeller angular velocity	300 RPM

Table 3. MAKO II Drivetrain Specifications

	Dimensions
Length	2578mm
Weight	43.5kg
Mounting points	8
Estimated Pilot Cadence	50 RPM
Sprocket Gear ratio	1:3
Bevel Gear ratio	1:2
Propeller angular velocity	300 RPM

Dividing the Drivetrain

To accommodate the revised pilot posture in MAKO II, the drivetrain was reconfigured into two sections: a front and a rear segment. The front segment was designed to house the pilot control interface, along with a lowered platform to support the pilot's forearms. The rear segment integrates the propulsion mechanisms, control outputs, and safety system. This modular arrangement enabled the removal of the intermediate drivetrain segment, which obstructed the pilot's revised posture within the hull.

Main Driver and transmission

The method chosen for pilot power input was a pedal-driven system comprising a crank, sprocket, and chain, similar to a bicycle. In MAKO I, the system utilized toe clip pedals; however, for MAKO II, the team adopted the use of cleats, due to cleats' compact form factor and improved ergonomics.

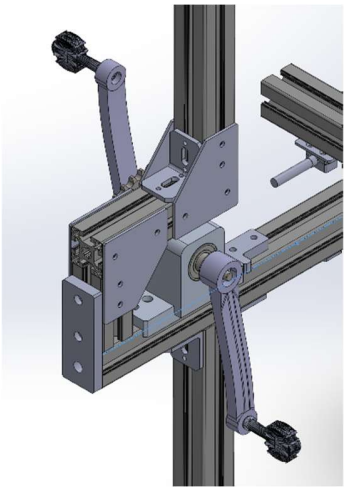

Figure 4: Pedal and Crank

Performance measurements from MAKO I's propulsion system indicated that the pilot could achieve a cadence of 50 RPM. The drivetrain configuration had a sprocket gear ratio of 1:3 and a bevel gear ratio of 1:2. This arrangement enables the system to convert the pilot's input rotation of 50 RPM to an output of 300 RPM at the propeller shaft.

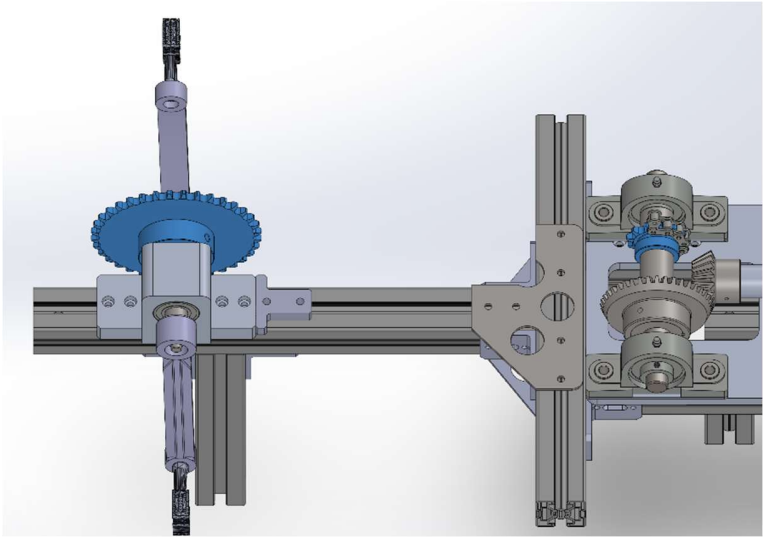

Figure 5: Sprockets

Addition of supports on the transverse and top of the drivetrain.

The drivetrain of the MAKO I featured four vertical profile supports connected to the bottom of the hull. For MAKO II, the forward section of the drivetrain was modified to contain four mounting points, and the aft section contains five supports on multiple axes to provide a robust and intact system under operational conditions.

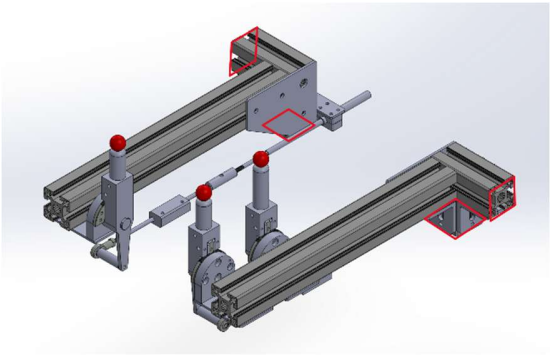

Figure 6: Forward Section Mounting Points

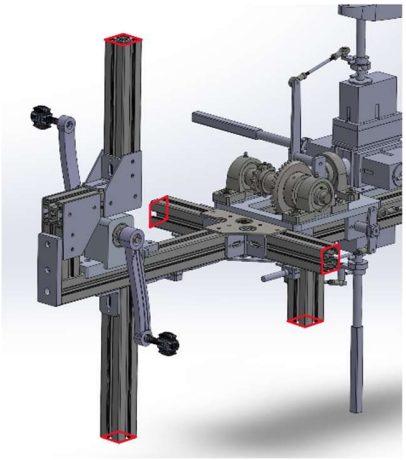

Figure 7: Aft Section Mounting Points

Further Optimization

After reviewing MAKO I design, the team saw opportunities to optimize the space and length of all components of the drivetrain. Therefore, the team reduced the space between the sprocket and bevel gear by 150mm, leading to a reduction in the length of the transmission chain.

Material

The material used in MAKO I's drivetrain consists of a combination of stainless steel, aluminium and cast iron. Components that are of high importance and those subjected to higher stresses are made of stainless steel (SS304). Aluminium was chosen as the primary material due to its lightweight properties and corrosion resistance. Therefore, aluminium extrusion profiles were used as the foundation

of the drivetrain. In addition, aluminium plates were utilized to provide a foundation to integrate the pillow blocks. To further optimise the weight, specific cutouts on the plates were designed. Balancing strength with structural integrity.

This hybrid approach to material selection led to multiple components rusting and degrading over time, which prompted a change for 2025's ISR. With the modification to the drivetrain, the rusted components were replaced with stainless steel components, ensuring the drivetrain's longevity and reliability.

3.2.2 Propulsor

Design

The main propulsor for our human-powered submarine consists of a single right-hand screw propeller, engineered for optimal thrust and manoeuvrability. In the early design stage, the basis was to produce an aero prop, as shown in the figure below. This was to ease the power required for torque generation ensuring pilot comfort. With the aero prop design, the blade area ratio (BAR) is reduced resulting in a decrease in drag compared to a standard Wageningen B series propeller. This allows the pilot to generate thrust easily as the required initial torque would be lower.

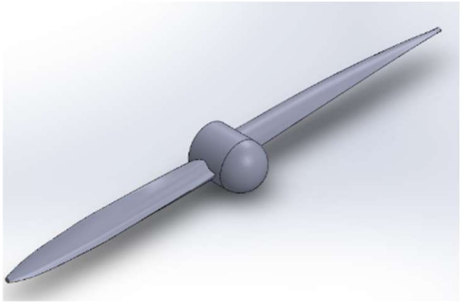

Figure 8: Aero Prop Model

However, using an aero prop presents several challenges. Firstly, there is notable inefficiency at low advance ratios (0–0.2), accompanied by a drop in efficiency at high advance ratios when operating at a fixed RPM. To mitigate this, aero propellers are typically designed with variable pitch, a feature that was not considered in this year's design. Secondly, aero props are designed to operate in air and placing them in water, which has a much higher density and viscosity than air, introduces substantial hydrodynamic loading that can lead to higher blade stress and fatigue. This increase in blade stress and fatigue can potentially lead to premature structural failure, which should be avoided. Therefore, after careful consideration, the final design will adopt a fixed-pitch B-series marine propeller, which is better suited to the operational conditions of the underwater human-powered submarine.

The Wageningen B-series propeller series offers configurations ranging from 1 to 8 blades [2], allowing naval architects to optimise propulsive performance based on specific operational requirements. In the previous iteration, MAKO I was designed based on a 4-bladed propeller. For MAKO II, however, a 2-bladed configuration has been selected to reduce hydrodynamic drag by minimising blade–water interaction. This change is expected to deliver better efficiency, particularly given the lightweight design and intended high-speed performance.

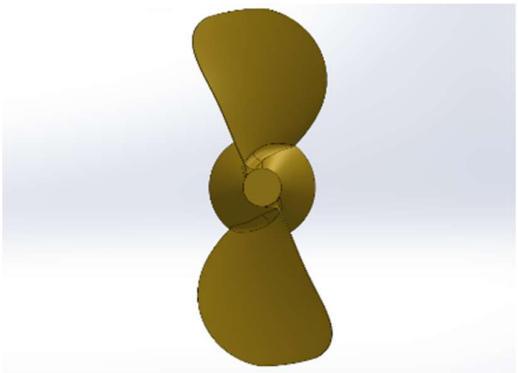

Figure 9: 2-Bladed B-Series Model

In addition to the previously mentioned reasons, several other factors support the decision to adopt a 2-bladed propeller for MAKO II. Generally, 2-bladed propellers offer advantages in terms of weight and cost. The lighter construction reduces overall system mass, which contributes to improved buoyancy and lowers manufacturing costs. For the MAKO II, which targets a rotational speed of 300 RPM (5 RPS), the reduced drag from a 2-blade design also lowers the torque required to maintain that speed since there is less blade area in contact with the water.

Table 4. Comparison between Propellers

Factors	2-Bladed B-Series	4-Bladed B-Series
Drag	Lower	Higher
Thrust Produced	Lower	Higher, particularly at high speeds
Efficiency	Higher	Lower
Weight & Cost	Lower	Higher

Numerical Simulations

With the design finalised, the 3D model was exported into STARCCM+. This generated numerical results for the propeller, such as open water efficiency, torque and thrust.

Table 5. Governing Parameters

Parameters	Values
RPS, n_s	2 rev/s
Density, ρ	998.67
Diameter, D_m	0.43m
Submarine Speed, V_s	4.63 m/s

In an open water propeller test, the primary parameter that is used to compare the inherent performance between propellers free of the ship's hull is the open water efficiency, which is written in Equation 1. However, there is another way to express it.

$$Open\ Water\ Efficiency, \eta_o = \frac{J}{2\pi} * \frac{K_T}{K_Q} \quad (6)$$

where

$$J = \frac{V_A}{n*D} \quad (7)$$

$$K_T = \frac{T}{\rho*n^2*D^4} \quad (8)$$

$$K_Q = \frac{Q}{\rho*n^2*D^5} \quad (9)$$

J is Advance Ratio; K_T = Thrust Coefficient; K_Q = Torque Coefficient.

To simulate the environment for open water testing, regions must be defined where the advance velocity (V_a) flow enters and exits the propeller stream. Anything outside of this region would be far field, or undisturbed flow. There are 4 main regions – upstream, static, rotating, and downstream. The upstream region is where the flow enters the stream, denoted by the V_a. Most of the flow are still uniform at this point, heading to the static region.

The static region would represent the fluid flow around the propeller, where fluid is disturbed due to the rotation of the rotation. The flow here is mostly turbulent and irregular. The rotating region is where the propeller is located, where the fluid flows through it. This is the most important region to denote, as the thrust and torque values are obtained here. The downstream region is where the fluid exits after passing through the propeller.

This simulation will replicate a steady, uniform flow field with a central stream, as defined by the region. The velocity of continua, which inputs the direction and flow velocity of the fluid, will be set as, $[-V_a, 0.0, 0.0]$. Where V_a is the speed of advance.
The rotating region will rotate along the x-axis at a revolution speed identical to the rotational speed of the propeller. This allows the region to rotate on the stationary propeller, simulating the rotation flow of the propeller.

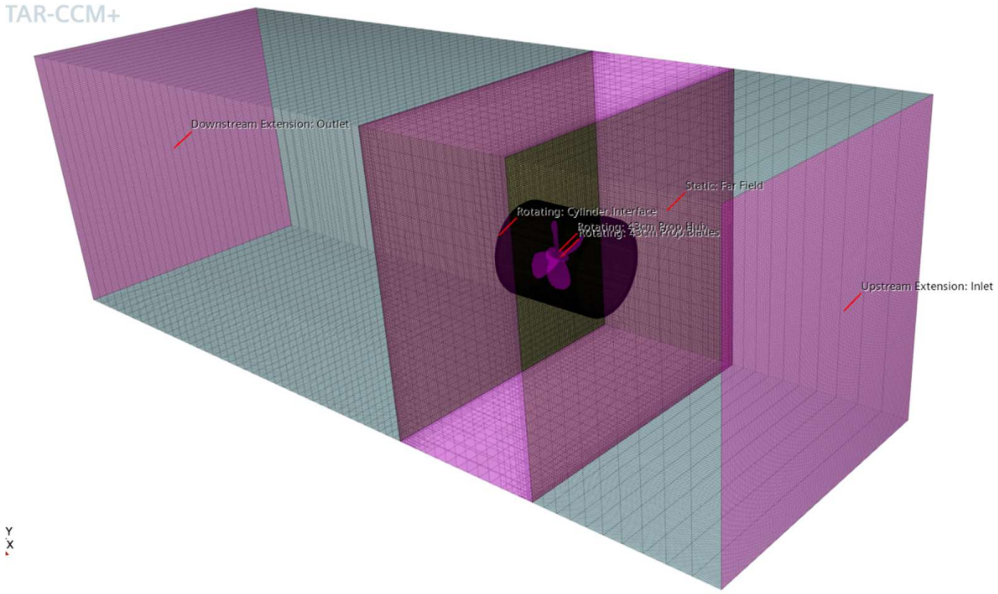

Figure 10: CFD Simulation on Propellers

Once the simulation is completed, the results are collated and displayed in the table below.

Table 6. Simulation Results

	Values
Peak Efficiency	0.6372 @ J = 1.078
Average Efficiency	0.4036
Average Thrust	482.1 N
Average Drag	831.19 N

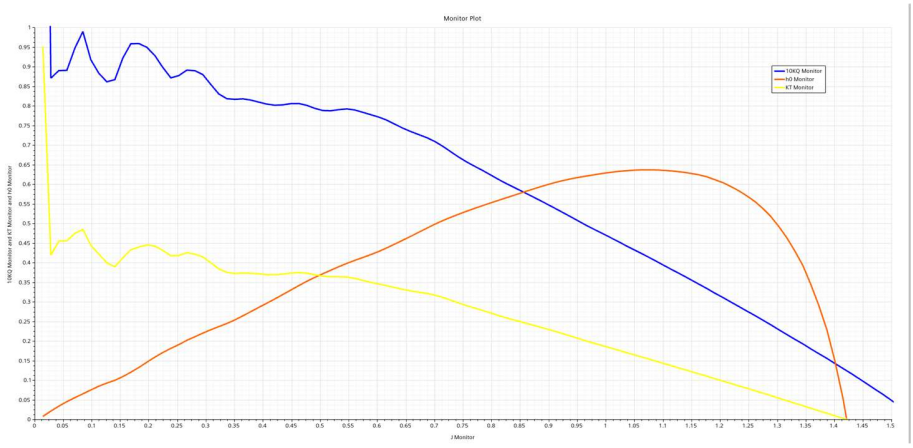

Figure 11: Open Water Efficiency vs Advance Ratio

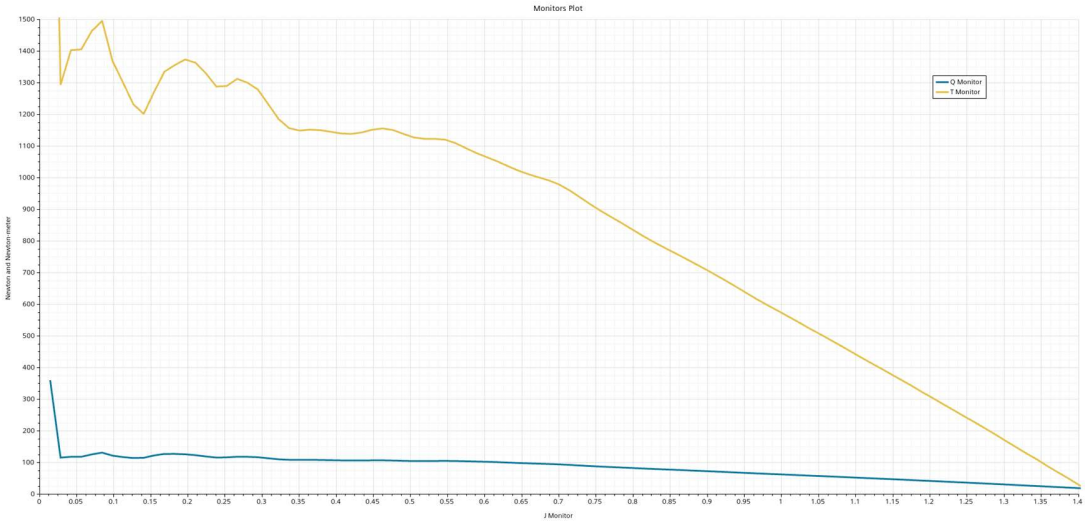

Figure 12: Thrust Against Torque

The design and fabrication process were carried out in close collaboration with our technical partner, Mencast, who specialises in production of marine propellers.

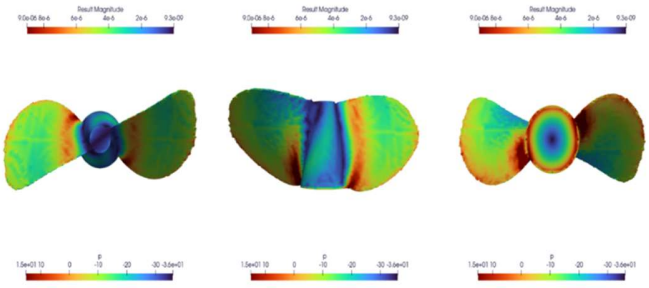

Figure 13: Pressure on the 2-Bladed Propeller using CFD (Part 1)

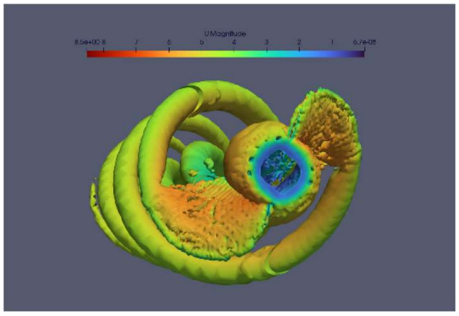

Figure 14: Pressure on the 2-Bladed Propeller using CFD (Part 2)

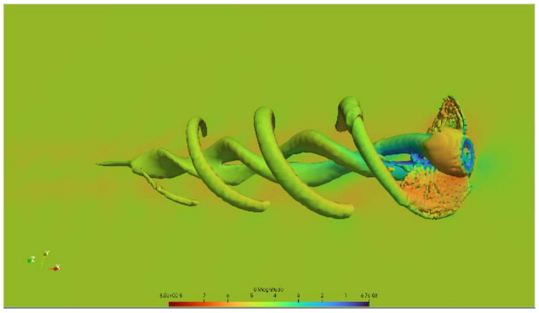

Figure 15: Pressure on the 2-Bladed Propeller using CFD (Part 3)

The figures above show the pressure distribution on a 2-blade propeller obtained through Computational Fluid Dynamics (CFD) simulations. The blue colouration represents the regions of low pressure, and the red colouration represents the regions of high pressure. As seen, there is no sudden change in pressure across the chord of the blade, only gradual changes. This proves to be effective in reducing the chance of cavitation and unnecessary stress on the propeller. The figures illustrate variations in pressure magnitude and total pressure across different blade orientations.

Fabrication with Mencast

Infill Pattern

The grill infill pattern was used for the 3D printing of the propeller, which provides strong vertical-axis support for the print. Although alternative patterns might offer higher overall strength, the grid infill provides a practical consideration between durability and efficient printing time.

Figure 16: 3D Printing of the 2-Bladed Propeller

Post-processing of the propeller

After 3D printing the propeller, post-processing was performed to enhance its surface finish and overall appearance. Polyester putty was applied for surface finishing. This post-processing technique not only improved the propeller's aesthetics but also contributed to better functionality by minimising surface irregularities.

For the process of applying the polyester putty, the propeller surface was thoroughly prepared before applying the putty to ensure optimal adhesion. This involved removing dirt and surface irregularities from the 3D-printed propeller by sanding to achieve a smooth and durable finish. The mixture was applied carefully to the surface of the 3D printed propeller by pressing the putty into the surface to avoid air bubbles. Once applied, the putty was left to dry completely. After the polyester putty was fully cured, the surface was sanded to achieve a smooth, uniform finish, contributing to improved performance and overall functionality.

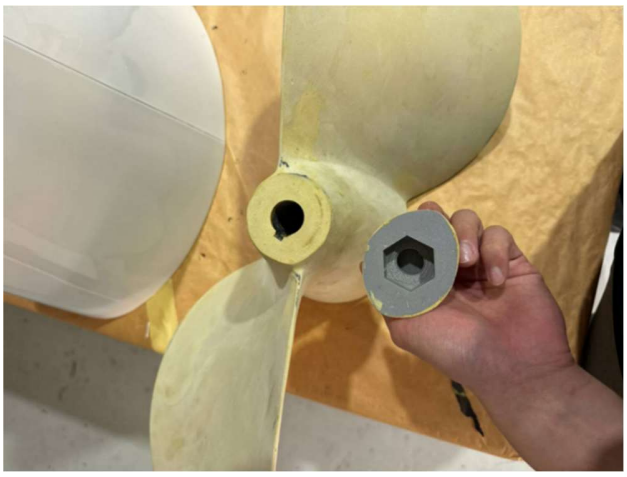

Figure 17: Applying Putty on the 3D Printed Propeller

Integration of Propeller to Drivetrain

A tapered shaft-to-propeller interface was employed to ensure a secure integration between the propeller and the drivetrain. To prevent rotational slippage and maintain synchronisation between the shaft and the propeller, a keyed shaft mechanism was incorporated. This mechanism involves a key that fits precisely into corresponding slots on both the shaft and the propeller, effectively locking them together as a single rotating unit.

Additionally, a boss cap with a right-hand threaded screw was installed at the end of the shaft. When tightened, the cap applies axial pressure, pushing the propeller onto the taper and further securing the connection. This design ensures that the propeller remains firmly attached to the shaft, even under conditions involving significant pressure and vibration.

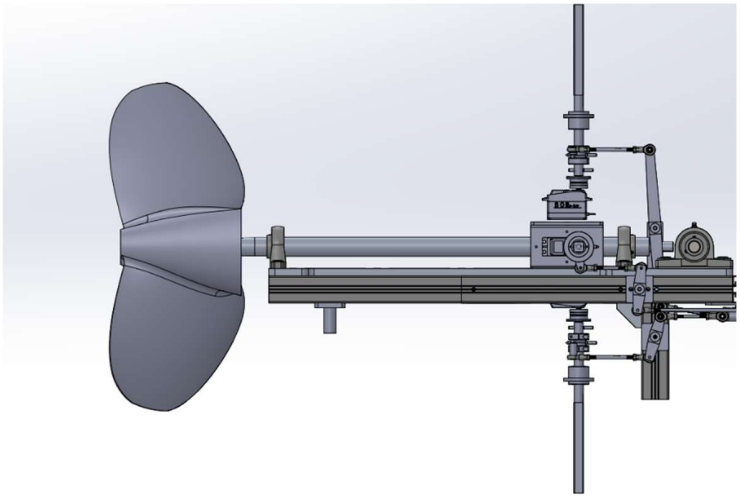

Figure 18: Integrating the Propeller to the Drivetrain

3.3 Hull

3.3.1 Hull Material Selection

The hull is constructed using a composite sandwich structure through the hand-lay-up method. It consists of a 1mm top and bottom layer of Quadriaxial QA-105 material, with a 3mm PET100 foam core in between. The core features a honeycomb-like hexagonal structure that enhances the strength-to-weight ratio, resulting in a total hull thickness of 5 mm.

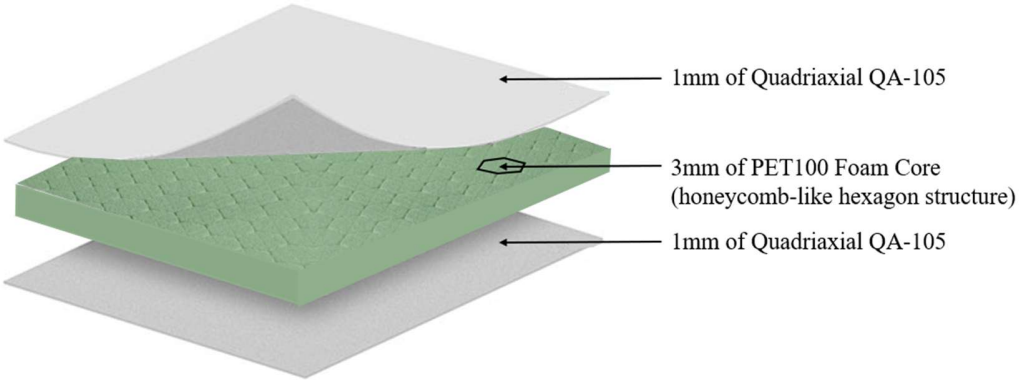

Figure 19: Composite Layer for the Hull [Easy Composites (2021)]

Figure 19 illustrates the cross-sectional view of the composite sandwich structure, which is designed for enhanced buoyancy and strength.

QUADRIAXIAL QA-1050

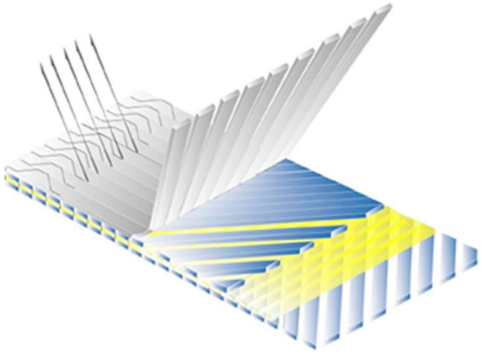

Figure 20: Quadriaxial QA-1050 Layers [Wee Tee Tong (2008)]

The decision to use QUADRIAXIAL QA-1050 for the hull construction was based on its mechanical performance. During the material selection process, QA-1050 emerged as the most suitable option for the hand lay-up process, particularly considering its application in a human-powered submarine. The material is easy to handle and suitable for complex curved surfaces, aligning with the design geometry of our hull. In addition, QA-1050 also offers good resin wet-out, allowing high laminate quality and minimize the formation of air pockets within the hull.

Additionally, the structure of QA-1050 provides quasi-isotropic properties, ensuring high mechanical strength and strong wet strength retention. These characteristics made it highly compatible with our chosen manufacturing method of hand lay-up process, contributing to both efficiency and performance. Overall, QA-1050 proved to be an ideal material that met both our structural and fabrication requirements.

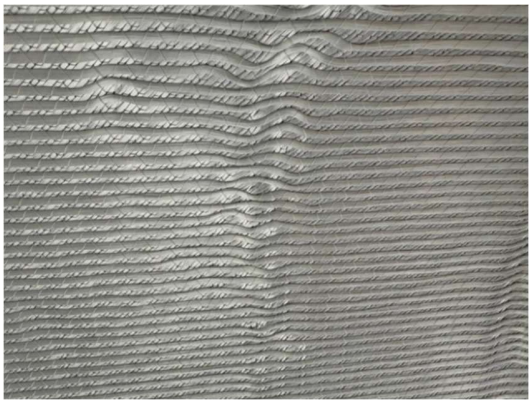

Figure 21: Quadriaxial QA-1050

Table 7: Fabrication Specifications (Part 1): Quadriaxial QA-1050

Layer orientation Degree [°]	0	+45	90	-45
Layer weight [g/m2]	272	256	270	256
[oz /y2]	8.0	7.6	8.0	7.6
Material	E-glass	E-glass	E-glass	E-glass

Table 8: Fabrication Specifications (Part 2): Quadriaxial QA-1050

Weight, knitting yarn	11 g/m^2
Weight, total	1054 ± 3% g/m^2
Standard roll width	126 cm
Standard roll length (approx.)	38 m
Standard roll weight (approx.)	50 kg

Table 9: Laminate Properties: Quadriaxial QA-1050

Matrix type	Fibre weight fraction	Fibre volume fraction	Layer thickness
Isophthalic polyester	54 [%]	35.6 [%]	1.3 [mm]

Table 10: Mechanical Properties: Quadriaxial QA-1050

Mechanical property	0°	+45°	90°	-45°
Tensile modulus [GPa]	15.7	18.2	16.5	15.4
Compressive modulus [GPa]	11.6	11.4	11.6	11.4
Tensile strength [MPa]	262	218	227	208
Compressive strength [MPa]	265	354	268	263
Elongation at break [%]	2.5	2.1	2.2	2.2
Shear strength, inplane [MPa]	135*	79*	141*	79*
Shear strength, interlam [MPa]	36.8	27.4	30.4	31.1

*Laminate Plate Theory calculations

PET100 Foam Core

The PET100 foam core was selected for its buoyancy and structural strength. Its honeycomb-like hexagonal structure allows it to conform easily to curved moulds, making it ideal for the geometry of our hull. The material also offers excellent mechanical properties and ranks among the top foam core options in terms of compressive and shear strength relative to its weight and density. The hexagonal structure promotes effective resin flow during the hand lay-up process, further enhancing laminate consistency and minimizing voids. This supported enhanced resin distribution and contributed to maintaining the lightweight design critical for an efficient human-powered submarine.

Figure 22: PET100 Foam Core [Easy Composites (2021)]

Table 11: Fabrication Specifications: PET100 Foam Core

Thickness [mm]	3
Resin Uptake [kg/m²]	0.938
Material	PET

Table 12: Mechanical Properties: PET100 Foam Core

Tensile Strength [MPa]	1.44
Tensile Modulus [GPa]	7.71
Compressive Strength [MPa]	8.23
Compressive Modulus [MPa]	3.16
Plate Shear Strength [MPa]	1.44
Plate Shear Modulus [MPa]	7.71
Density [kg/m³]	95

Benefits of Using a Honeycomb Core Structure

Honeycomb structures are a type of design featuring a hexagonal core. This "sandwich effect" from the core significantly enhances the bending stiffness of the overall hull, making it ideal for applications like human-powered submarines, where high strength-to-weight ratios are critical for performance efficiency. A lightweight structure is beneficial for the performance of a human-powered submarine, as it helps reduce energy consumption while maintaining structural integrity.

Hull Thickness & Strength Calculations

Determining the thickness is a crucial factor in the preliminary design phase, as it significantly impacts the weight and strength of the submarine. The goal was to find the optimal balance by determining the minimum thickness required to support the weight of the submarine, while keeping it as light as possible. To obtain that, the maximum bending stress acting on the hull must be calculated.

Firstly, the points where the force is acting on the hull must be measured and recorded relative to a datum located on the aft end of the drivetrain. The supporting points are determined by where the hull comes into contact with the cradle.

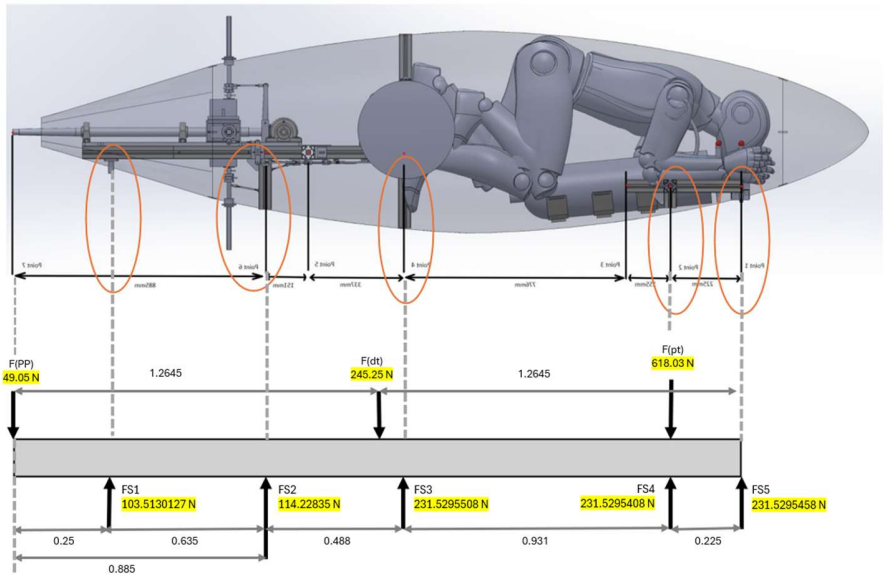

Figure 23: Simple Beam Diagram

As the resulting supporting forces are unknown, the gaussian elimination method was used to find the values.

Table 13: Gaussian Elimination Calculation

							Moment of Propeller	Moment of Drivetrain	Moment of Pilot
Point 1	0	$1Fs_2$	$1Fs_3$	$1Fs_4$	$1Fs_5$	=	49.05	245.25	618.03
Point 2	$-0.64Fs_1$	0	$0.488Fs_3$	$1.419Fs_4$	$1.644Fs_5$	=	-43.41	34.7	876.98
Point 3	$-1.12Fs_1$	$-0.488Fs_2$	0	$0.931Fs_4$	$1.156Fs_5$	=	-67.34	34.7	575.39
Point 4	$-2.05Fs_1$	$-1.419Fs_2$	$-0.931Fs_3$	0	$0.225Fs_5$	=	-113.01	-193.62	0
Point 5	$-2.28Fs_1$	$-1.644Fs_2$	$-1.156Fs_3$	$-0.22Fs_4$	0	=	-124.05	-248.81	-139.06

Table 14: Supporting Reaction Forces

Reaction Forces	Newtons (N)
F1	103.51
F2	114.23
F3	231.53
F4	231.53
F5	231.53

With all the forces solved for, the simple beam theory can be used to find the maximum bending moment, $BM = 222.3Nm$

With continuous iterations, the thickness used to find the second moment of area is $Iz = 0.000020963m^4, Iy = 0.000617437m^4$. The difference in vertical and horizontal inertia is due to the ovular shape of the cross-section, where the semi-major and semi-minor axes differ in length.

Using the beam formula $\sigma = \frac{My}{I}$, the maximum stress the hull will encounter is $\sigma y = 1829.31Pa,\ \sigma x = 621.082Pa$

Thus, the hull thickness is sufficient as the maximum stress is < material yield strength, $\sigma = 208Mpa,\ where\ \sigma x, < \sigma$.

3.3.2 Hull Design

Establishing Design Requirements

The design process started by establishing the primary goals and objectives for this year's competition. Through a structured voting process, it was determined that the foremost objective would be to achieve the maximum possible speed for the submarine.

Design constrains

Based on experiences from European International Submarine Races (eISR), the need to reduce the submarine's overall profile was highlighted. This was to minimize shipping costs and volume by adopting a fully modular design approach. The hull is divided into four main components: canopy, top hull, bottom hull, and aft cone. Additionally, key systems such as the drivetrain, control fins, and propeller are designed to be detachable and shipped separately. All modular components can be reassembled using a standardized system of bolts and fasteners, enabling efficient transport, maintenance, and reconfiguration.

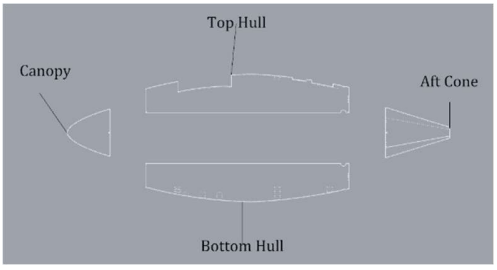

Figure 24: Exploded View of Hull

3D modelling and CFD Optimization

To optimise the hull design, over 50 3D models were developed using SolidWorks and Rhino 3D. This approach enabled the use of parametric design techniques, allowing the team to systematically refine the hull's geometry by applying a set of equations to achieve an optimal hydrodynamic shape (Khan, Sher., 2018).

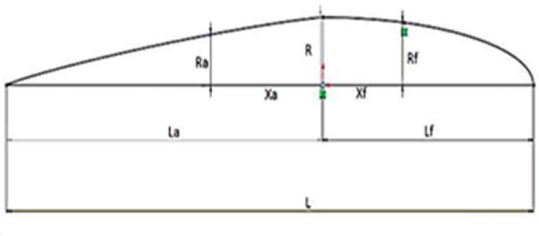

Figure 25: Hull Form Parameters

The equation of the curve of the forward body is given as

$$R_f = R\left[1 - \left(X_f/L_f\right)^n\right]^{\frac{1}{n}} \quad -(1)$$

The equation of the curve of the after body is given as

$$R_a = R[1 - (X_a/L_a)^n]^{\frac{1}{n}} \quad -(2)$$

Table 15. Parametric Values of a selected few Hull Models

Hull	Length	Ratio of Horizontal Width to Bow	Ratio of Vertical Height to Bow	Horizontal Diameter	Vertical Diameter	n Number Forward	n Number Aft	Volume	Surface Area
E	2.9	0.3	0.5	0.6	0.7	1.7	1.5	0.52	4.46
F	2.9	0.3	0.45	0.56	0.7	1.7	1.5	0.48	4.52
G	2.9	0.3	0.48	0.56	0.7	1.7	1.5	0.49	4.53
H	2.9	0.3	0.45	0.58	0.7	1.7	1.5	0.50	4.60
I	2.9	0.3	0.45	0.58	0.7	1.7	1.4	0.48	4.07
Mako I	3.6	0.4	0.4	0.56	0.7	1.7	1.5	-	-

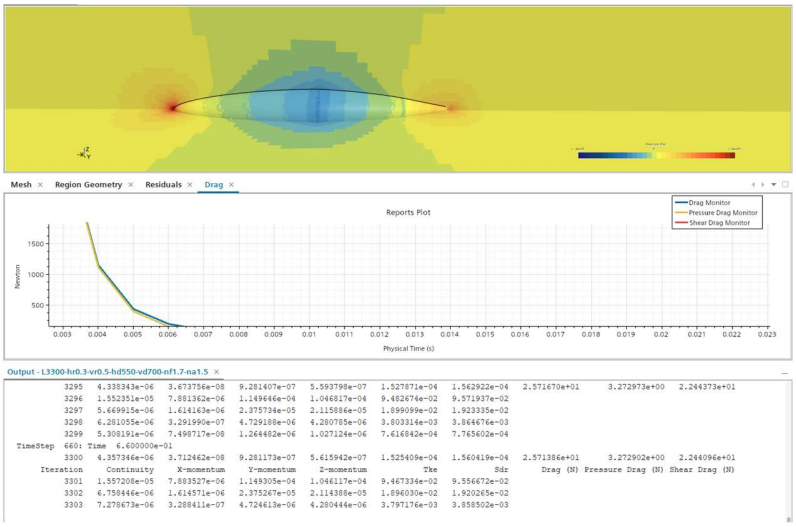

Figure 26: CFD Simulation of Hull

After designing and evaluating the initial hull models, Computational Fluid Dynamics (CFD) simulations were conducted to assess hydrodynamic performance. The analysis revealed that surface area is the primary contributor to drag in a fluid-filled human-powered submarine. As a result, design efforts were focused on minimizing surface area while maintaining sufficient internal volume to ensure pilot functionality and comfort.

Table 16. Mako I Simulation Results

Hull	Drag(N) at 5 Knots	Drag(N) at 9 Knots
Mako I	51.04	175.05

Table 17. Mako II Simulation Results

Hull	Drag(N) at 5 Knots	Drag(N) at 9 Knots	Drag at 5 Knots (%)*	Drag at 9 Knots (%)*	Surface Area
E	51.04	153.96	- 11.96	-12.05	4.46
F	48.94	148.012	-15.58	-15.45	4.5
G	49.05	148.28	-15.40	-15.29	4.53
H	49.93	145.93	-14.00	-13.86	4.60
I	49.18	148.5	-15.17	-15.13	4.07

*Comparison with Mako I

From the initial set, the top five models were selected for further evaluation based on five key criteria: pilot fit, required drivetrain modifications, drag reduction, internal volume, and total surface area. This multi-criteria assessment enabled a balanced approach to selecting a final hull design that optimised both performance and usability.

To evaluate the pilot's fit within the hull, a human mannequin replicating the pilot's anthropometric dimensions was modelled and positioned inside the submarine. Spatial constraints were then assessed based on this setup. Additionally, to ensure the pilot's pedalling motion would not be impeded, a maximum revolution envelope was generated around the pilot's knees and legs to simulate the full range of cycling movement

Table 18. Hull Selection Matrix

		Hull #E		Hull #F		Hull #G (selected)		Hull #H		Hull #I	
Criteria	Weight	Rating	Weighted Score	Rating	Weighted Score	Rating	Weighted Score	Rating	Weighted Score	Rating	Weighted Score
Space for Pilot	4	5	20	3	12	5	20	5	20	3	12
Space for Drivetrain	3	3	9	2	6	3	9	2	6	3	9
Drag reduction %	3	1	3	5	15	4	12	2	6	3	9
Internal Volume	2	1	2	5	10	3	6	2	4	4	8
Surface Area	1	4	4	3	3	2	2	1	1	5	5
Total			**38**		**46**		**49**		**37**		**43**

Table 19. Difference between Hulls

Hull #E	Hull #F	Hull #G (Chosen)	Hull #H	Hull #I
No protrusion, Slight larger overall size compared to G	Negligible protrusion	No protrusion, compared with H: G is larger at the forward section	No protrusion, larger volume, compared with G: aft is larger at the aft section	Similar to E: slight protrusion for pedalling radius, aft is slightly sharper compared to E
Significant increase in vertical distance, slight increase in horizontally	Significant increase in vertical distance, slight reduction horizontally	Significant increase in vertical distance, horizontally ok	Significant increase in vertical distance, slight increase horizontally	Slight increase in vertical distance, slight decrease horizontally

Taking all evaluation criteria into account, Hull G was selected as the final design. It demonstrated the most favourable balance between hydrodynamic efficiency and functional requirements. Hull G provided a significant reduction in drag, accommodated the pilot with minimal drivetrain modifications, and maintained an optimal balance between internal volume and surface area, making it the most suitable choice for further development and fabrication.

3.3.4 Integration and Evaluation

Following the simulation phase, a 15% reduction in hydrodynamic drag was achieved compared to the previous year's hull design.

Upon completion of all simulations, the integration of all submarine components was carried out, during which additional modifications were identified for the drivetrain.

Furthermore, a custom 3D-printed drivetrain mount was designed to facilitate secure attachment to the hull. This mount provided both structural stability and ease of removal, thereby enabling efficient maintenance operations.

Trim, Hydrostatics & Stability

The submarine is designed to be slightly negatively buoyant, allowing for the addition of foam to adjust buoyancy as needed.

Table 20: Buoyancy

	Volume	Buoyancy Force (N)	Weight (N)	
Hull	0.0273	267.87	254.89	$1Fs_5$
Pilot	0.06522	639.81	657.27	$1.644Fs_5$
Drivetrain	0.006188	60.704	245.25	$1.156Fs_5$
Air Tank	0.022	215.82	196.2	$0.225Fs_5$
Propeller	0.02	196.2	49.05	0

Longitudinal Centre of Gravity (LCG) = 1.3033m from Aft

Vertical Centre of Gravity (VCG) = 0.2386 from baseline

Longitudinal Centre of Buoyancy (LCB) = 1.5894m from Aft

Vertical Centre of Buoyancy (VCB) = 0.2976m from baseline

An important condition for submarines is that the VCG is below the VCB, where 0.2976m > 0.2386m (condition met)

3.4 Control Surfaces

3.4.1 Introduction

The submarine is designed to operate at a depth of approximately 6 meters, with the primary objective of achieving maximum velocity in a straight-line drag race. To maintain stability and allow for minor adjustments in terms of trim and roll, the submarine is equipped with control fins. The selected fins will be crucial for ensuring the submarine remains on course and responds effectively to any necessary manoeuvring inputs.

3.4.2 Aerofoil Profile Considerations

In the previous submarine design, the primary design priority was manoeuvrability, which significantly influenced the selection of the control fin aerofoil profile. After evaluating multiple symmetric NACA profiles, the NACA 0018 was chosen for its balanced aerodynamic performance. This profile demonstrated a favourable lift-to-drag ratio at low angles of attack, a relatively high stall angle, and sufficient structural thickness to accommodate the mechanical mounting system. Furthermore, the NACA 0018 profile was advantageous from a design-to-manufacture perspective, as its publicly available coordinate data facilitated accurate and efficient modelling in SolidWorks, thereby streamlining the transition from design to fabrication.

The design objectives established for the 2025 competition were revised to focus on straight-line, high-speed performance. In line with this purpose, the team examined the aerodynamic benefits of using a narrower, symmetrical aerofoil, notably the NACA 0012, due to its potential for lower drag. A comparative analysis was performed against the previously implemented NACA 0018 to determine whether the transition could result in measurable performance improvements while maintaining the submarine's stability and control, particularly during unexpected course deviations that may occur under race conditions

3.4.3 Reynolds Number Calculation

$$Re = \frac{\rho * V * L}{\mu}$$

$$Re = \frac{995.41 \times 4.6296 \times 0.24}{0.001138}$$

$$= 9.77 \times 10^5$$

ρ = Density of water = 999.97 kg/m³
V = Velocity = 4.6296 m/s (Assuming peak velocity is at 9 knots)
L = Chord length = 0.24 cm
μ = Dynamic viscosity of water = 0.001138 Pa·s (Dynamic viscosity of water assumed to be at 15°C)

The Reynolds Number of 9.77×10^5 falls within the fully turbulent flow regime. Although moderate in comparison to large-scale marine applications, this value is sufficiently high to expect the development of turbulent boundary layers along the control surfaces. Such flow conditions will have a significant impact on lift, drag, and stall behaviour, particularly when comparing different foil thicknesses. Based on the Reynolds number calculated using assumed parameters, aerodynamic coefficient data for both the NACA 0012 and NACA 0018 profiles were obtained from the Aerofoil Tools database, which compiles results from XFOIL simulations and experimental studies. The data include both lift and drag coefficients as functions of angle of attack (α). These results were plotted, as shown in Figure 27, across a range of angles of attack from 0° up to the onset of stall, to allow a direct comparison of the two profiles under identical Reynolds number conditions.

3.4.4 Comparing NACA Profiles

Looking at the graph above, at small angles of attack (0° to 5°), both NACA 0012 and NACA 0018 perform similarly, with a lift slope of around 0.1 per degree. As the angle increases, NACA 0018 starts to show better performance, reaching a maximum lift coefficient of about 1.42 at 18°. NACA 0012 peaks slightly lower at around 1.39, with its maximum occurring a bit earlier, at about 17°. Although both profiles stalls at similar angles, NACA 0012 has a sharper drop in lift after stall, making it harder to maintain control over its stability.

In terms of drag, NACA 0012 shows slightly lower drag at low angles because of its thinner profile. However, as the angle of attack increases past 10°, its drag increases more steeply, and its lift drops off faster. NACA 0018 has slightly more drag at small angles, but it handles stall more smoothly, keeping a more stable lift to drag ratio beyond 10°.

Both profiles perform best between 6° and 10°, where their lift to drag ratios are highest. NACA 0012 might reach a slightly higher peak efficiency, but that quickly drops after stall. On the other hand, NACA 0018 keeps its performance more stable beyond the peak, which is helpful if the submarine moves slightly outside the ideal control range.

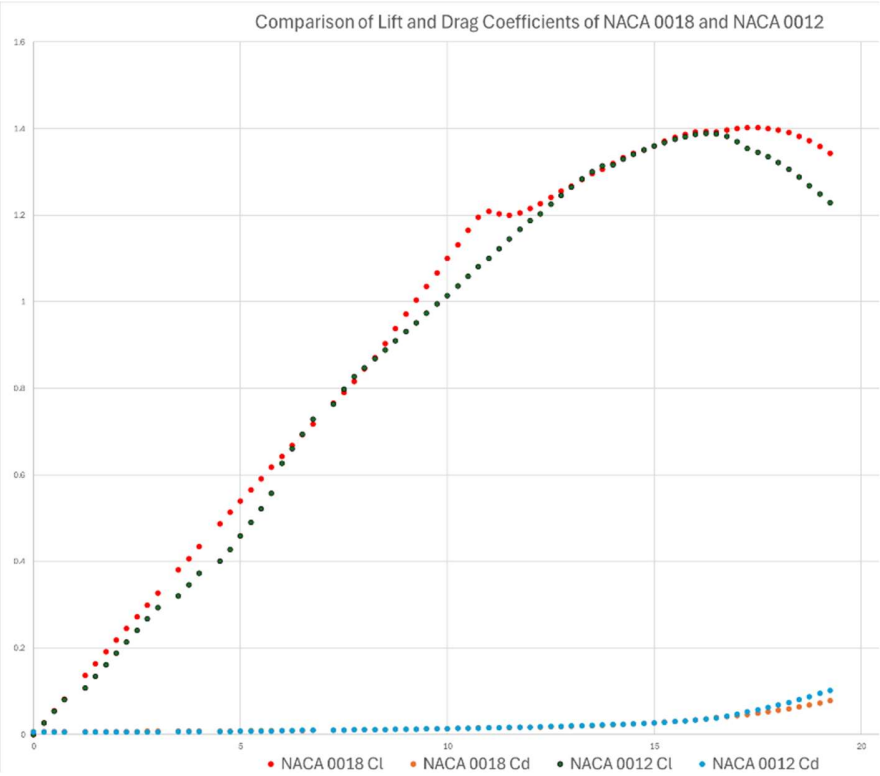

Figure 27: Comparison of Lift and Drag Coefficients for NACA 0018 vs NACA 0012

To further evaluate aerofoil performance by referring to existing CFD results and studies, regarding NACA 0012 and NACA 0018, relevant simulations were reviewed [1]. The results, shown in Figure 29, indicate that NACA 0018 generates a greater pressure differential across its surface, as seen in the stronger blue region on the suction side and the red region on the pressure side. This results in higher lift. Its thicker profile also produces smoother velocity gradients shown in the red to orange region in the velocity contours, which provides a better flow and a delayed stall. In contrast, NACA 0012 shows a sharper red velocity region and a more symmetric pressure distribution. While this suggests slightly higher peak velocity, it also indicates sharper flow acceleration, making it more prone to early flow separation and sudden stall. For our submarine control fins, where post-stall stability and consistent lift are important for both straight line performance and emergency manoeuvring, NACA 0018 offers better hydrodynamic reliability and is therefore the more suitable choice for the 2025 ISR design.

Figure 28: NACA 0012 (Left) and NACA 0018 (Right) Thickness Comparison

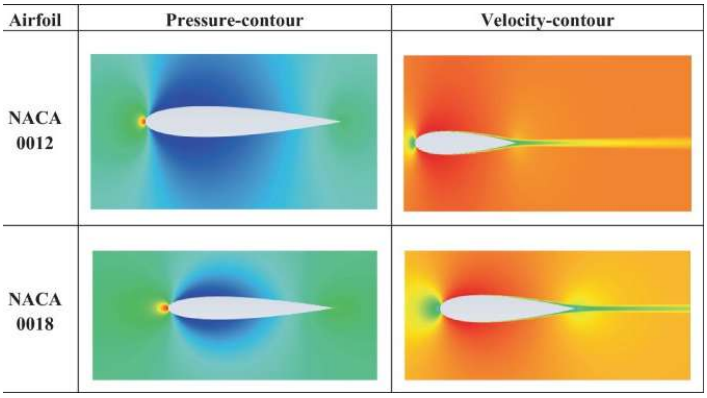

Figure 29: NACA 0012 and 0018 Pressure-Velocity Comparison [1]

3.4.5 Control Fins Design

After selecting the NACA 0018 aerofoil for its favourable lift characteristics and stable stall behaviour, the control fin geometry was scaled down to 80 percents of its original size used last year. This decision was made to match the overall reduction in the submarine's dimensions. As the current hull design is smaller than that of the previous year, scaling down the fins ensures proportionality between the control surfaces and the revised hull plan. This is necessary to maintain consistent hydrodynamic performance, as retaining the original fin size on a smaller hull could result in excessive control sensitivity, increased drag, and disrupted flow patterns around the stern.

Each control fin is mounted using an M5 tapped hole located through the tip of the fin, allowing it to be directly fastened to the metal actuation shaft (control shaft). This configuration provides a strong and secure mechanical interface, preventing any rotational slippage or misalignment under hydrodynamic loading. It also allows for easy disassembly and reinstallation during maintenance or tuning. The fins were fabricated using PLA via 3D printing, with four perimeter walls and a 60% gyroid infill pattern, chosen to maximise bending stiffness while minimising weight.

To assess water absorption, a trial fin piece was soaked in a bucket of water for over two hours. The mass increased from 300.3 g to 307.8 g, indicating a water uptake of only 2.5%. However, this was an uncoated sample. The final fins underwent surface smoothing and were coated with paint, which significantly reduces surface porosity and limits water seepage. Therefore, any minor absorption in the printed PLA core is expected to have a negligible impact on buoyancy or hydrodynamic performance, especially over the short-duration races of the ISR. The coating would act as a protective barrier and combined with the high infill density and enclosed shell, the fins remain water-resistant throughout operation.

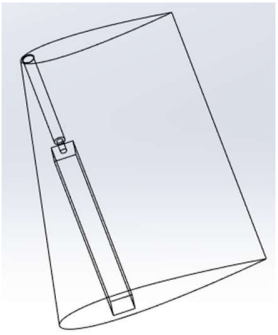

Figure 30: Final Wireframe Design of Control Fins

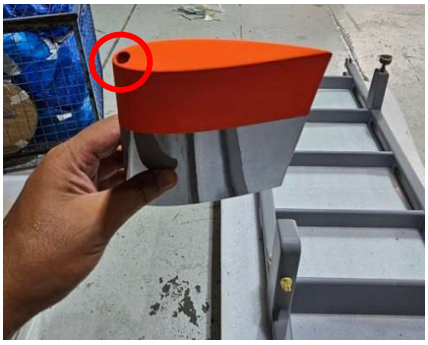

Figure 31: M5 Hole for Securing Control Fin to Rod

3.4.6 Control Fins Mounting

In the previous year's submarine design, the control fins were mounted directly onto the hull, which resulted in a visible gap between the fin base and the curved surface. This gap was caused by the difficulty of installing the control fin bearing on a curvature surface. To overcome this limitation, the team tested various bonding compounds in an attempt to attach the bearing to the hull securely.

For the current design, a new control fin mounting bracket was 3D designed and printed to conform precisely to the curvature. This modification provides a smoother transition between the fin and the body, thereby improving the hydrodynamic performance by reducing local turbulence and enhancing flow attachment. Aesthetically, it also creates a more integrated appearance.

The mounting bracket consists of two mirrored parts, which allows for efficient 3D printing and ensures symmetrical installation on both sides of the hull. These components were fabricated using PLA, selected for its ease of use, wide availability, and suitability for rapid prototyping. Once printed, the two halves are assembled around a ball bearing housed within the mount. This integrated bearing enables smooth and controlled rotation of the fins, significantly enhancing the responsiveness and precision of the submarine.

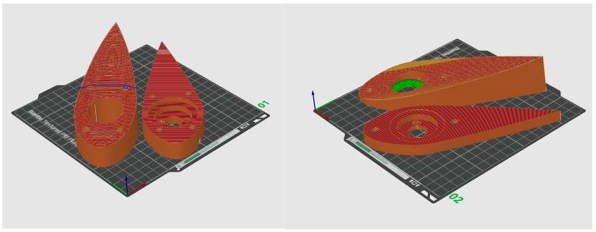

Figure 32: 3D Print of the Control Fins mount

Figure 33: Control Fins Integrated with the Mount

3.5 Mechanical Controls

3.5.1 Input mechanism

The method used in MAKO I to control the angle of the control fins was by the manual actuation of levers at the front of the drivetrain. The decision was made for MAKO II to keep the levers as the main actuation mechanism for the pilot, as it serves as a reliable method of control with a low probability of failure.

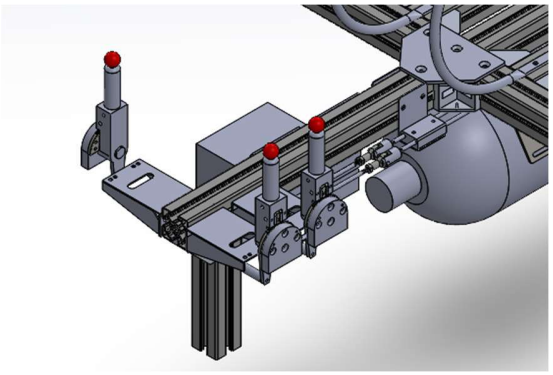

Figure 34: MAKO I Pilot Control

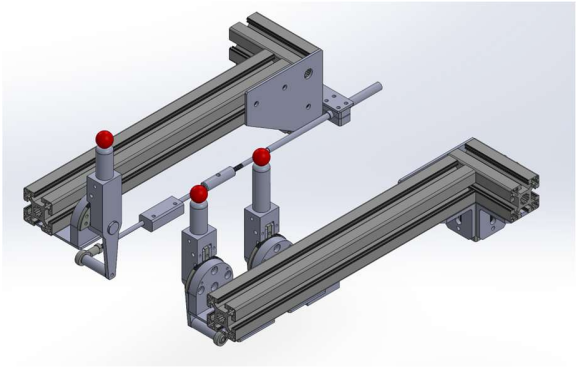

Figure 35: MAKO II Pilot Control

3.5.2 Control Rods & Mechanical Linkages

In MAKO I, the actuation of the control levers at the front of the drivetrain was transmitted via the use of mechanical linkages along the longitudinal profile of the drivetrain onto the control rods, where the control fins are connected. However, this approach was unfeasible for MAKO II due to the segmentation of the drivetrain, which introduced a discontinuity between the forward and aft sections. As a result, the team had to devise a solution to transmit the pilot controls from the forward to the aft.

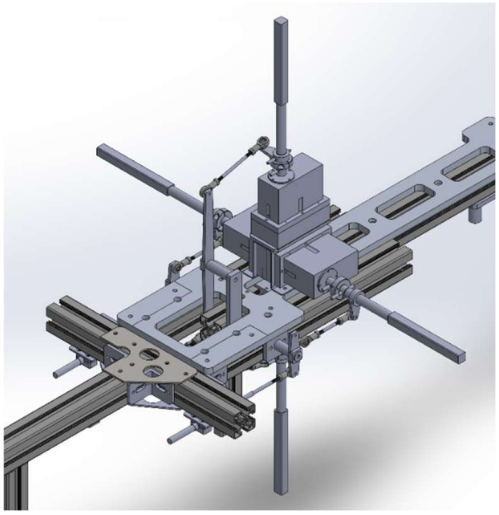

Figure 36: Control Rods with Linkages

3.5.3 Push-pull cables

The solution selected for transmitting control from the front of the drivetrain for the MAKO II was the implementation of push-pull cables. This solution provides greater design flexibility, allowing the cables to be routed along the bottom side of the hull towards the aft section, where the control rods and fins are located.

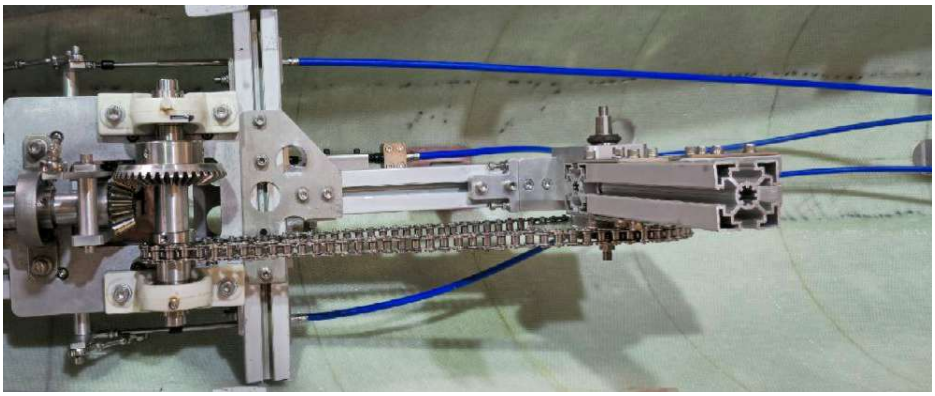

Figure 37: Push Pull cables at Aft Section (Top View)

3.6 Electronic Control System

3.6.1 System overview

The two objectives for the electronic control system were to monitor the submarine's operational state during runtime and provide a dual control method over the submarine's manoeuvrability. The system design focused on the principle of modularity by segregating functions into different modules to achieve compartmentalisation and abstraction of responsibilities for each module.

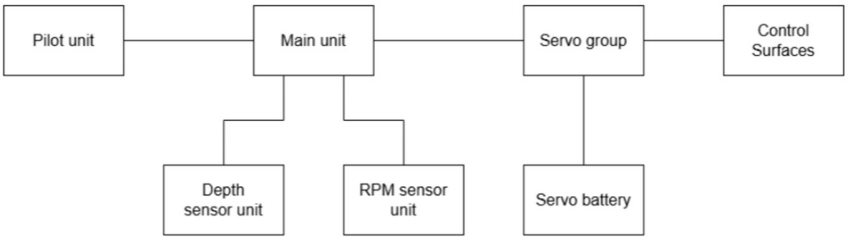

Figure 38: Electronic Control System Diagram

The monitoring system is implemented through an integrated network of sensor units deployed throughout the submarine, providing sensor data readings to the main unit, which houses the MCU for data aggregation and processing. The sensor network continuously tracks four key parameters to represent the submarine's state: speed over ground, current depth, compass heading, and propeller shaft RPM. The system employs a three-axis accelerometer and magnetometer to obtain speed over ground and compass heading, and a barometric pressure sensor to obtain current depth readings. The propeller shaft's RPM is sensed using an infrared optical sensor that detects reflective strips positioned on the propeller shaft. The aggregated telemetry data is then displayed in the pilot unit to improve the pilot's awareness and stored in a local external storage device for further data analysis.

The dual control method comprises two operational modes: automated and manual. In automated mode, the main unit performs calculations based on sensor readings to generate control signals for the servo group, which consists of four servo motors responsible for each control surface. This mode would allow the pilot to concentrate on pedalling while the system maintains the course. The manual mode serves as the primary fail-safe mechanism, activated by the pilot in the event of an automated system malfunction requiring pilot intervention. In this mode, pilot inputs are captured through a dedicated interface unit, processed by the MCU, and subsequently executed by the servo group.

3.6.2 Prototyping

The prototyping phase comprises two key developments: the electronic system and the enclosure. The electronic system development focuses on designing and refining the core monitoring and control system emphasizing system reliability and robustness. While the enclosure development addresses the critical challenge of the operating environment to provide protection for the electronic system from water ingress, while maintaining accessibility for maintenance.

The electronic system development process adopted a modular implementation strategy, mirroring the system's design principle.

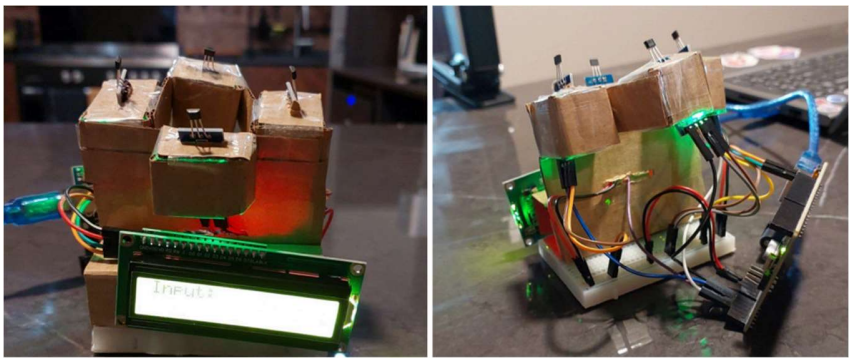

Figure 39: Pilot Unit Prototype

The pilot unit prototype demonstrates the successful integration of electronic components designed to facilitate pilot-system interaction, incorporating four hall-effect sensors to enable a two-axis joystick control alongside an LCD interface that provides real-time visualization of essential sensor data for environment awareness.

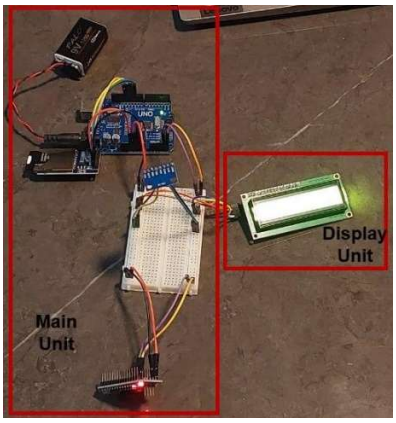

Figure 40: Main Unit Prototype with Display Connection

The main unit prototype showcases the system integration of core computational and data processing components, incorporating a combined three-axis accelerometer and magnetometer assembly for motion sensing and implementing data logging capabilities through persistent storage on external media.

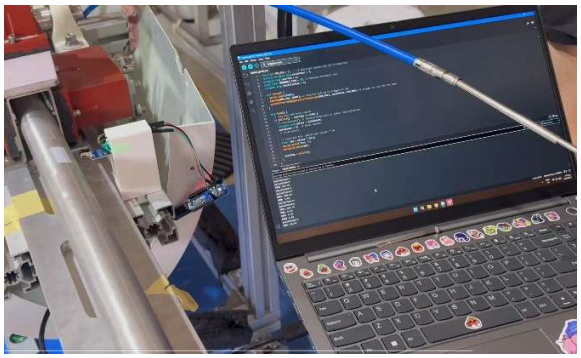

Figure 41: RPM Sensor Prototype

The RPM sensor unit underwent calibration and functional verification testing under controlled conditions on land. While such validation cannot fully replicate the underwater operating environment, this preliminary testing phase successfully confirmed the fundamental operational integrity of the monitoring system architecture prior to underwater deployment.

The enclosure development process followed an iterative approach to create a waterproof housing to protect the electronic components. Initial prototyping iterations addressed both form factor and functionality, with each subsequent version incorporating improvements based on the results of previous testing and evaluation. Additionally, to minimise the impact on the submarine's buoyancy, the system design methodology restricted the use of air-filled enclosures, using them only when necessary. Where possible, electronic components should be potted in epoxy resin.

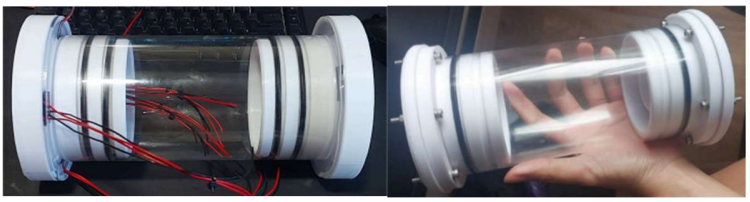

Figure 42: Main Unit Enclosure Prototype Version 1 (left) and Version 2 (right)

Figure 43: Final Main Unit Version

The main unit necessitated an air-filled enclosure to ensure proper functionality of its electronic components. Following two complete design-test iterations that involved prototyping, pressure testing, and performance evaluation, a technical assessment revealed that procuring a commercially available enclosure solution from BlueRobotics offered superior time efficiency and reliability, leading to the adoption of this off-the-shelf alternative.

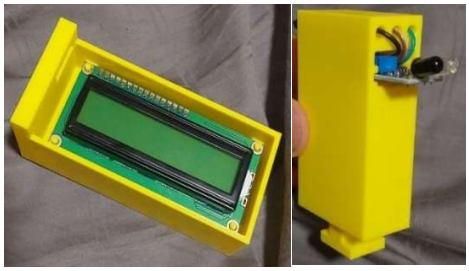

Figure 44: LCD Display Housing (left) and IR Sensor Housing (right)

For the auxiliary electronic components, it was determined that resin potting represented an optimal solution, enabling cost-effective production of interchangeable modules to support operational requirements for quick component replacement. This design approach provided significant advantages for subsystems by combining robust environmental protection and field-serviceable modularity.

3.6.3 Challenges

Despite rigorous development efforts, the waterproof enclosure for the main unit proved unsuccessful after multiple iterations, with persistent water ingress issues remaining unresolved despite thorough root cause analysis. These enclosure failures impeded electronic system development by preventing realistic operational testing, with setbacks attributed to insufficient execution planning, limited manpower, and an overly ambitious project scope. While the electronic control system demonstrated theoretical feasibility in concept and design, the cumulative implementation challenges resulted in the incompletion of a fully functional prototype.

3.7 Safety Systems

3.7.1 Rules

In accordance with the International Submarine Race (ISR) Contestant Manual, Section 6.5.6 under Submarine Safety Requirements, all competing submarines must include a deployable safety buoy system. This buoy must be secured to the hull using a highly visible tether and be designed for rapid deployment in the event of an emergency. Its primary function is to alert rescue divers to the submarine's location, and it must be released via a fail-safe mechanism commonly referred to as a "dead man's switch." To meet this requirement, the team has engineered a custom mechanical dead man's switch system that integrates a bicycle brake handle with a pawl and ratchet mechanism, enabling reliable and immediate buoy deployment in the event of pilot loss of control or consciousness.

3.7.2 Dead man's Switch Design

The system utilises a metallic brake cable housed within a rubber outer sleeve, which is connected to an assembly. Upon release of the brake handle by the pilot, a tensioned spring lifts the pawl, thereby disengaging the ratchet mechanism. This enables rapid deployment of the safety buoy, which ascends freely to the surface due to its inherent buoyancy, effectively alerting the safety divers.

Initial development included a mock-up of the ratchet mechanism, which was 3D modelled using SolidWorks to visualise the assembly and test spatial constraints. The first physical iteration was fabricated using PLA through 3D printing. Despite testing with 100% infill and various internal structures, physical stress and strain tests consistently revealed mechanical failure under load. Hence, the design was revised using 3 mm aluminium plates, and both the baseplate and pawl were handcrafted, as illustrated in Figure 46. For improved rotational performance, ball bearings were integrated into the 3D-printed ratchet system.

To facilitate secure storage and consistent deployment, the buoy will be housed in a 3D-printed holder equipped with multiple drainage holes at its base. A cable sleeve is also implemented to guide the string smoothly during freewheeling of the ratchet as the buoy is released. This holder design minimises water accumulation and ensures buoy stability during operation, thereby reducing the risk of entanglement or interference with the drivetrain.

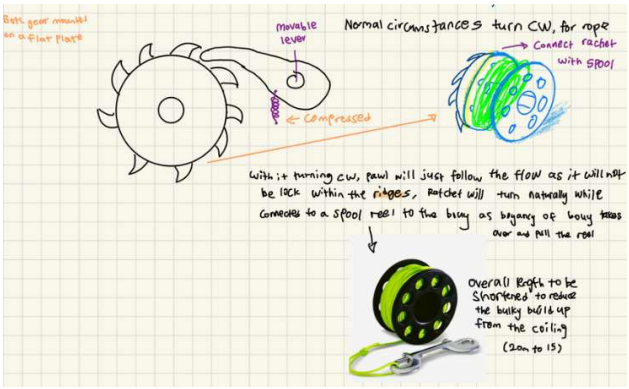

Figure 45: Rough Design Sketch of the Safety System

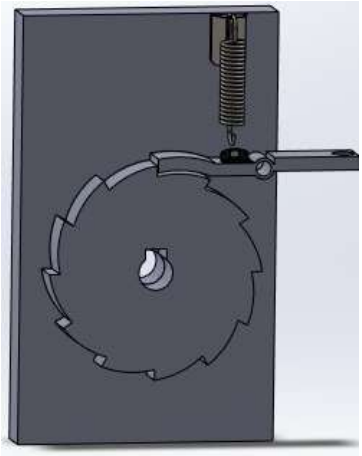

Figure 46: 3D Model Mock-Up

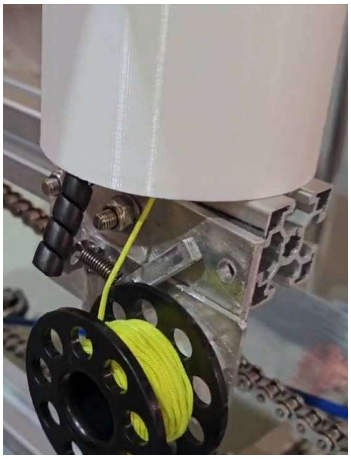

Figure 47: Cable Sleeve

3.7.3 Safety Buoy

The buoy itself is an off-the-shelf fishing trawl float, selected for its high buoyancy and quick ascent properties, which are critical in emergency scenarios. The entire system is designed for reliability, safety, and rapid activation, all while ensuring it does not disrupt submarine performance during normal operation. The buoy also meets the competition requirement of at least 4” in the smallest dimension, with the selected size being 4.5” in diameter.

Figures 48 and 49: 3D Printed Buoy Housing with Drainage Hole

3.7.4 Strobe light

The XTAR SD1 scuba diving strobe beacon was selected based on its compact form factor, high luminous output, and proven waterproof performance. These characteristics directly addressed the primary design requirements for the submarine's strobe light system, enabling effective visual signalling while minimizing hydrodynamic interference with the hull's profile. To ensure all-around visibility during

operation, beacons were integrated into the hull at four cardinal positions: dorsal, ventral, port, and starboard surfaces. Implementation involved fitting custom 3D-printed mounting assemblies into cutouts of the hull, which provided secure fixture points while maintaining the structural integrity. This configuration achieved the balance between operational visibility requirements and preservation of the submarine's hydrodynamic efficiency.

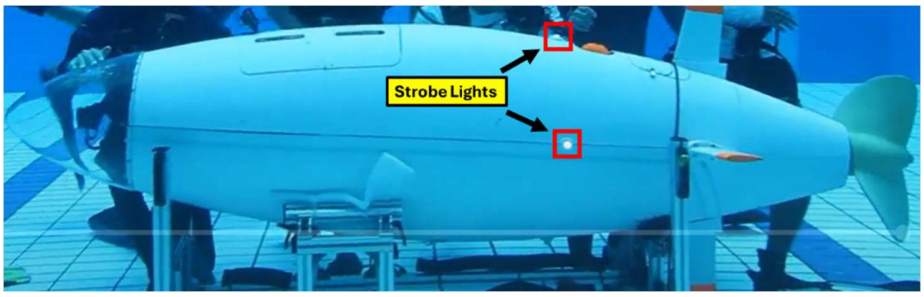

Figure 50: Strobe Lights on MAKO II

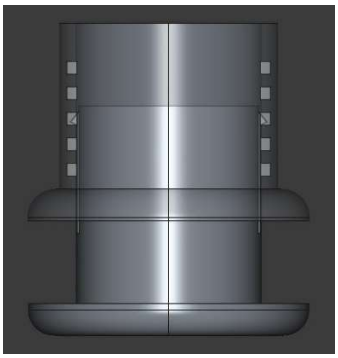

Figure 51: Side Profile of Strobe Light Mount in 3D Model

The strobe light mounting system employs a two-component design comprising of a male and female component to achieve a secure attachment to the hull while maintaining hydrodynamic efficiency. The male component installs with its planar surface flush against the exterior hull, while its protruding feature extends inward to interface with the female clamping mechanism. This configuration was deliberately engineered with a flat hull interface surface to optimize manufacturing consistency during 3D printing processes and facilitate replication across multiple units. Although the mount's compact dimensions naturally minimize the effects of hull curvature, the design incorporates multiple adjustable latching receptacles to accommodate potential variations in hull thickness while maintaining structural integrity. Particular attention was given to hydrodynamic performance, with the external surface profile featuring filleted edges to reduce drag coefficients. The strobe light aperture was dimensioned to provide the necessary illumination intensity while presenting minimal frontal area disruption to the water flow. This balanced approach successfully addresses the competing requirements of secure mounting, manufacturing practicality, and hydrodynamic efficiency in the design solution.

4. Summary of Design Options

MAKO II was developed through a comprehensive evaluation of multiple design iterations, with emphasis on practicality, performance, and manufacturability. Each design component was assessed using computational modelling, material testing, and ergonomic analysis to achieve an optimal balance of hydrodynamic efficiency, pilot comfort, and mechanical durability.

Hull Design Variants

More than 50 hull configurations were generated and analysed using Star-CCM+ simulation software. Among them, Hull G emerged as the optimal choice, demonstrating a 15.3% drag reduction at a cruising speed of 9 knots. This design successfully balanced hydrodynamic performance with functional requirements by preserving sufficient internal volume for the pilot and drivetrain. Additionally, the incorporation of a PET100 foam core enabled neutral buoyancy, further enhancing the hull's efficiency and stability.

Propulsion Configuration

A 2-bladed Wageningen B-series propeller was selected over a 4-bladed alternative due to its lower hydrodynamic drag and greater efficiency at approximately 300 RPM. The propeller was 3D printed in-house using a grid infill pattern to enhance structural strength. Post-processing was then applied to achieve a smooth surface finish, further optimizing hydrodynamic performance.

Control Surface Profiles

Among the tested NACA aerofoils, NACA 0018 was selected over NACA 0012 due to its higher stall angle of up to 18° and superior structural rigidity. These characteristics provided improved stability under turbulent flow conditions and enhanced manoeuvrability during International Submarine Race (ISR) trials.

Drivetrain Transmission

MAKO II adopted cleat pedals to replace the toe-clip system used in MAKO I, resulting in improved pedalling efficiency and greater pilot control. A 1:6 gear ratio, implemented through a sprocket-to-bevel gear mechanism, optimized torque transfer to the propeller. To enhance mechanical robustness and ease of servicing, modular frame supports were incorporated, streamlining drivetrain maintenance and improving overall system reliability.

Material Considerations

The hull employed a sandwich composite structure composed of QUADRIAXIAL QA-1050 fiberglass layers, a 3 mm PET100 foam core, and Epicote 1006 resin for bonding. This configuration significantly improved both buoyancy and structural integrity. Stainless steel components replaced the previously used aluminium for drivetrain and propulsion mounts, offering greater corrosion resistance. Additionally, 3D-printed mounts enabled precise integration with the hull, effectively minimizing mechanical vibrations and enhancing overall drivetrain stability.

The MAKO II design is a testament to the team's dedication to refining underwater vehicle technology. By prioritising hydrodynamic efficiency, pilot ergonomics, and manufacturing feasibility, the team ensured that every decision was based on rigorous testing and real-world constraints. This meticulous approach not only met performance benchmarks but also positioned the vehicle as a strong competitor in the International Submarine Race. The result is a high-performance craft that strikes a balance between cutting-edge engineering and practical execution.

5. Test & Trials

The comprehensive testing and validation of the MAKO II submarine represented a critical phase in confirming design viability, functional performance, and operational safety prior to international deployment. Thanks to Singapore Polytechnic and the Naval Diving Unit from the Republic of Singapore Navy, the test program translated theoretical insights and design models into tangible, real-world readiness, pilot integration, and control systems under varying operational conditions.

5.1 Test Locations & Timeline

To ensure MAKO II's operational readiness and safety, a series of controlled pool trials were conducted across two locations:

Singapore Polytechnic (SP) Pool
Dates: 24, 28, 29, 30 April; 2, 8, 15, 16 May 2025
Environment: Shallow-depth pool (≤ 2 m)
Objectives: Conduct initial buoyancy assessments, evaluate control surface responses, and perform propulsion system trials.

Naval Diving Unit (NDU) Training Pool, Sembawang Camp
Dates: 4, 10, 11 May 2025
Environment: Deep-water facility (10 m operational depth)
Objectives: Validate deep-water performance, execute full-scale safety protocols, and carry out pilot recovery exercises in realistic conditions.

These progressive tests provided valuable data that informed design adjustments and confirmed system performance under both controlled and simulated operational conditions.

The phased program progressed through:

- Phase I (24–30 April): Static systems testing
- Phase II (1–10 May): Dynamic propulsion and control validation
- Phase III (11–16 May): Final integration checks, pilot training, and safety simulations

5.2 Testing Objectives

The testing process for MAKO II is designed to comprehensively evaluate its performance, structural integrity, safety systems, and operational readiness for underwater deployment. A primary objective involves assessing the effectiveness of communication and coordination between the pilot, support divers, and land-based control teams. Clear and reliable communication is imperative to ensure operational coherence, particularly during complex manoeuvres and potential emergency situations. Effective information exchange among all parties enhances situational awareness and contributes significantly to safety and mission success.

Structural integrity testing constitutes a significant component of the evaluation process. Given the modular nature of the hull, it is essential to confirm its capacity to endure varying hydrodynamic forces and operational loads. Controlled testing conditions are employed to verify the security of structural joints and to observe material behaviour under extended submersion. These assessments inform refinements to the hull design, ensuring its durability and resilience in both competitive and real-world scenarios.

The attainment of neutral buoyancy is critical for stable propulsion and precise manoeuvrability. By adjusting buoyancy parameters under different aquatic conditions, the team aims to optimise balance and control responsiveness while minimising hydrodynamic drag. This process directly supports energy efficiency and ensures consistent performance across varied test environments.

Finally, the validation of safety mechanisms and emergency protocols is integral to ensuring the preparedness of the pilot and support personnel. All safety systems—both internal and external—are subjected to rigorous testing, including simulated escape procedures and recovery drills. These exercises are conducted under realistic conditions to evaluate response times and procedural effectiveness. The outcomes of these tests serve to confirm the reliability of the emergency systems and enhance the overall safety framework of the vehicle.

5.3 Methods & Procedures

This section outlines the experimental procedures undertaken to evaluate the operational readiness, safety, and hydrodynamic performance of the MAKO II prototype. The methods were designed to simulate real-world conditions and ensure compliance with safety and performance benchmarks.

5.3.1 Buoyancy & Trim Testing

Initial testing focused on assessing the buoyancy and trim characteristics of the MAKO II. Trim control was refined through the manual repositioning of foam and weighted blocks along the vehicle's structure. Divers conducted visual inspections at the fore, midship, and aft sections to monitor the distribution and make iterative adjustments. These procedures ensured longitudinal stability and neutral buoyancy under both static and dynamic conditions, forming the foundation for subsequent in-water trials.

5.3.2 Pilot Entry, Exit & Safety Simulations

Pilot ingress and egress protocols were evaluated through a series of timed simulations conducted under both standard and stress-induced conditions. The trials emphasized the following key aspects:

- Optimization of the pilot's cycling posture to facilitate rapid exit
- Functional integration of the dead man's switch with the safety buoy system
- Execution of simulated incapacitation drills to assess emergency response protocols

Foam-assisted flotation was tested at the Naval Diving Unit (NDU) Pool, where live rescue scenarios were rehearsed in coordination with certified divers, medical personnel, and lifeguards. These simulations validated the effectiveness of the safety systems and ensured that emergency procedures could be executed reliably under realistic conditions.

5.4 Findings & Adjustments / Challenges Encountered

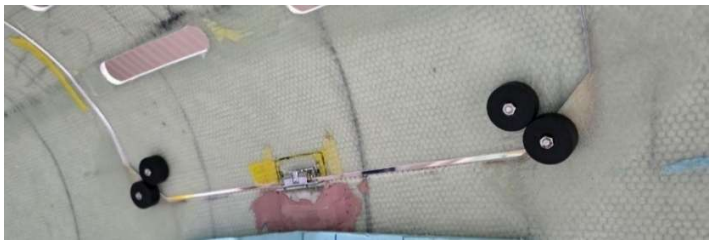

Figure 52: Pilot Hatch and Magnet Integration

Pilot Hatch Retention Enhancement:

During multiple operational test runs, the pilot hatch cover demonstrated a recurrent tendency to dislodge due to the dynamic cyclic movements associated with pilot ingress, egress, and in-situ adjustments. Inadvertent upward pressure from the pilot's lower back either during pedalling or while repositioning frequently compromised the hatch's secure placement. To address this issue, an industrial-grade neodymium magnet retention system was introduced. These magnets delivered a high holding force capable of maintaining hatch closure under typical operational stresses, while still allowing for rapid manual disengagement in emergency situations. This design solution effectively reconciled the dual requirements of secure mechanical retention and immediate accessibility, thereby improving both operational robustness and pilot safety.

Figure 53: Bow Foam Placement

Buoyancy Optimization in the Pilot Compartment

Neutral buoyancy within the pilot compartment was achieved through the strategic placement and minimization of buoyant foam. Instead of uniformly distributing the foam throughout the compartment, its application was selectively optimized to deliver the required buoyant force while avoiding excessive material that could introduce unnecessary structural weight or increase hydrodynamic drag. This targeted approach ensured that the submarine maintained neutral buoyancy under operational conditions, thereby improving overall stability and manoeuvrability without compromising performance efficiency.

Ergonomic Integration of Buoyancy Elements

To maintain both neutral buoyancy and pilot efficiency, foam blocks were strategically placed within the pilot compartment to avoid interfering with leg movement while pedalling. Iterative modifications were made during the installation procedure to ensure that buoyant materials did not infringe on the kinematic envelope required for efficient pedalling. Pilot fatigue was reduced, and effective propulsion was supported by this meticulous spatial optimization, which preserved ergonomic clearance while maintaining the required buoyant force. The final design successfully integrated weight distribution, hydrodynamic performance, and operating comfort.

Safety Buoy System Reliability Enhancement

Numerous unintended deployments of the safety buoy system occurred during several trial sessions, which were attributed to rust in the release mechanism. Specifically, under operating conditions, early activation resulted from rusted components that impaired the mechanical linkage's integrity. To address this problem, the release mechanism was redesigned to increase reliability, and all affected parts were replaced with corrosion-resistant substitutes. These changes significantly reduced the likelihood of inadvertent deployment,

thereby strengthening the system's operational robustness and ensuring that the safety buoy only operates under specified emergency situations.

Canopy Ventilation Optimization

In submersion tests, air was regularly observed to accumulate under the canopy, which negatively impacted the submarine's trim and the pilot's forward vision. Due to insufficient ventilation, trapped air was able to change the centre of buoyancy and upset the hydrodynamic balance, causing this problem. More ventilation holes were added to the canopy to address this issue and facilitate regulated air release during descent. However, the initial pattern of perforations proved to be excessive, causing stress concentrations that weakened the canopy and jeopardized its structural integrity. Fortunately, with three extra canopy units on hand, the team ran a series of controlled tests to examine different hole designs. An ideal pattern was identified that successfully reduced air entrapment and maintained the canopy's mechanical strength under operating loading conditions through iterative refinement.

Figure 54: Canopy

5.5 Final Performance Summary

- MAKO II Reliability: No structural failures recorded (no significant damages)
- Total Underwater Trial Hours: 52 hours
- Standard Daily Testing Duration: 6.5 hours (9:00 AM – 3:30 PM)

Table 21. Number of Underwater Trial Hours

	Total Scheduled Days	Estimated Fully Usable Days	Estimated Partially Usable Days (50%) due to bad weather	Total Hours
SP Pool	8	4	4	(4 × 6.5) + (4 × 3.25) = **39 hours**
NDU Pool	3	1	2	(1 × 6.5) + (2 × 3.25) = **13 hours**
				= **52 hours**

*Average Emergency Egress Time Recorded: **15-20 seconds**

The full-scale emergency egress drills conducted by the SIT Nautical Knights team at the NDU Training Pool played a crucial role in validating safety protocols and assessing the effectiveness of pilot responses. By simulating scenarios such as pilot incapacitation, injury, and mechanical failure, the team ensured preparedness for potential real-world incidents.

Each drill was meticulously timed, capturing the interval between the initial emergency trigger and the moment the pilot surfaced and signalled the safety officer on land. This approach enabled a thorough assessment of reaction time, situational awareness, and the execution of coordinated emergency responses. The 3-meter depth provided a controlled yet challenging environment to test mobility, extraction techniques, and communication between divers and land support teams. These rehearsals were integral to refining procedural efficiency and ensuring rapid intervention in critical situations.

5.6 Pilot's Surface Air Consumption (SAC)

5.6.1 Definition & Importance

Surface Air Consumption (SAC) refers to the rate at which a diver consumes air at surface pressure (1 ATA). Measured in litres per minute (L/min), it provides a baseline to estimate air consumption at various depths.

Tracking the pilot's SAC is critical for

- Operational safety – estimating the pilot's available bottom time and ensuring sufficient air supply.
- Emergency preparedness – enabling accurate reserves for surfacing in case of propulsion failure or system malfunction.
- Performance monitoring – identifying stress or fatigue through abnormal consumption patterns during multiple trials.

5.6.2 Methodology & Assumptions

Cylinder Type: Standard AL80 (11.1 L)

Conversion: 1 bar × 11.1 L = air consumed (in litres)

Dive Depth: 10 meters → Ambient pressure = 2 ATA

SAC Formula:

$$SAC = \frac{(P_{start} - P_{end}) \times V}{t \times P_{Ambient}}$$

Where:

P = Pressure in bar
V = Tank Volume
t = Time in minutes

5.6.3 Record of SAC

11 May 2025 – Dive Trials at NDU:

Table 22. Surface Air Consumption (Part 1)

Run	Start Bar	End Bar	Time (min)	Air Used (L)	SAC (L/min)
1	120	115	1.50	55.5	18.5
2	115	100	1.34	166.5	62.1
3	100	95	2.36	55.5	11.8
4	95	85	2.15	111.0	25.8
5	85	75	1.45	111.0	38.3

After the fifth run, the team decided to replace the air tank to reset the buoyancy.

Table 23. Surface Air Consumption (Part 2)

Run	Start Bar	End Bar	Time (min)	Air Used (L)	SAC (L/min)
6	200	190	0.35	111.0	79.3
7	190	180	0.47	111.0	58.9
8	170	150	2.36	222.0	47.0
9	150	130	2.07	222.0	53.6

5.6.4 Observations

- Most efficient SAC: Run 3 (11.8 L/min) during steady propulsion at moderate effort.

- Highest SAC: Run 6 (79.3 L/min), likely due to crash conditions or stress response.
- SAC Range: Between 11.8 – 79.3 L/min, depending on workload, environment, and stress level.
- Operational average: For standard runs (1–5, 8–9), SAC values mainly remained between 18–53 L/min,

The MAKO II test program confirms the submarine's readiness for ISR 2025, with performance, safety, and integration metrics exceeding internal benchmarks. As the first Southeast Asian team to compete at ISR, this testing phase signifies not only engineering achievement but also regional representation in the global submarine innovation.

6. Arena. Construction, Maintenance & Repair

6.1 Project Fabrication Overview

The hull design for Mako II was intentionally shortened and lightened compared to Mako I, reflecting a strategic shift in focus from manoeuvrability to speed optimization. The Mako II human-powered submarine was entirely developed and fabricated by undergraduate students at the Singapore Institute of Technology (SIT), under the mentorship and technical guidance of Integrated Coating Solutions (ICS). This collaborative project functioned as an experiential learning platform that fostered design thinking and iterative problem-solving by integrating advanced digital design tools with hands-on manual fabrication techniques. By bridging theoretical knowledge with practical implementation, the initiative enabled the team to develop both specialized technical competencies and essential professional skills, including teamwork, communication, adaptability, and project management.

Material/Method	Description
Plywood (6mm thickness)	Provided a structurally stable base and framework for the mould, ensuring dimensional accura formation.
Veneer (1mm thickness)	Applied in multiple layers to produce a smooth, fair surface on the mould, critical for achieving high-quality composite layup and precise hull geometry.
Laser-cut wooden station profiles	Fabricated from SolidWorks designs to precisely define the hull's cross-sectional geometry, enabling accurate spatial alignment and consistent mould shape.
Quad axial fiberglass	Served as the primary reinforcement material, offering multidirectional mechanical strength essential for withstanding complex hydrodynamic loads on the submarine hull.
Epoxy resin	Selected for its superior bonding properties, mechanical strength, and environmental durability, ensuring long-term performance and integrity of the composite structure.
Awlfair (marine fairing compound)	Used to correct surface irregularities on the mould, providing a seamless finish necessary for optimal laminate adhesion and hydrodynamic efficiency of the final hull.
Gloss black paint	Applied as a sealing and inspection layer on the mould surface, facilitating defect detection an composite layup.
3D Printing	Employed to produce complex, custom components with high precision, enhancing design flexibility and integration of non-standard parts in the submarine assembly.
Soric foam core	Incorporated within the composite layup to enhance stiffness and facilitate resin distribution without substantially increasing weight.

6.2 Material Summary

6.3 Fabrication of Hull mould

Frame structure

The fabrication of Mako II began with the production of a negative mould, essential to ensure that the final hull met design specifications and exhibited a smooth, fair surface. The team's prior experience with this technique, combined with its proven reliability, informed the selection of this traditional boatbuilding method. Compared to more advanced techniques such as resin infusion, the negative mould

approach was more time-efficient and cost-effective, aligning better with the project's available resources and skill sets. Resin infusion was deemed less suitable due to its requirement for complex machinery and a steeper learning curve. With a shared understanding of the chosen methodology, the team proceeded with constructing the mould. An inverse hull design was generated using SolidWorks to develop the negative mould geometry shown in Figure 56. This model enabled the hull to be segmented into discrete station profiles, which were subsequently converted into laser-cut templates. By targeting a tolerance of ±5% throughout production, the team ensured high dimensional accuracy while significantly reducing human error during the early fabrication stages.

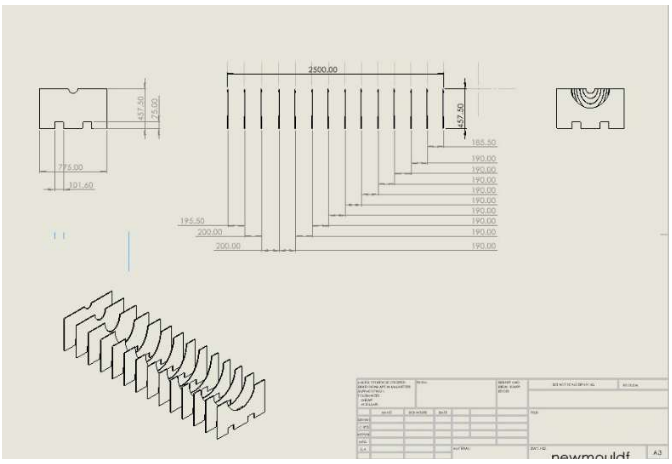

Figure 55: SolidWorks Station Profile

Once the laser-cut station profiles were ready, two parallel aluminium beams were installed as the foundation for the mould. The aluminium beams, measuring 2300 mm in length and 100 mm in width, provided a rigid and stable framework that guaranteed precise alignment and maintained the mould's structural integrity throughout fabrication. To further stabilize the profiles, L-brackets were used to mechanically fasten the aluminium beams, preventing lateral or vertical displacement during assembly.

Figure 56: Station Mould Framework

Achieving positional precision along the principal axes required a systematic inspection of each frame using spirit levels to assess vertical, horizontal, and diagonal orientations. This alignment procedure was essential for maintaining the intended hull geometry and minimizing the accumulation of errors throughout the composite layup process. To reinforce the structural integrity of the levelled framework, plywood strips were carefully affixed in both horizontal and diagonal configurations across sets of three or more profiles, thereby forming a triangulated brace. This arrangement substantially increased stiffness, reduced deformation, and ensured consistent profile positioning. As a result, the developing hull retained dimensional fidelity during fabrication, culminating in a fair and geometrically precise form that adhered to the project's design tolerance of ±5%.

<u>Hull Structure</u>

The hull of Mako II was constructed utilising a shipbuilding technique known as cold moulding. This involved the application of plywood strips, each approximately 20 mm in width and 5 mm in thickness, hand-laid across a minimum of three adjacent station profiles.

This method was intentionally chosen to facilitate the natural formation of the hull's curvature while mitigating internal stresses commonly induced by forced bending, achieving a monocoque structure.

These plywood strips enabled the structure to distribute mechanical loads evenly across the working surface areas, thereby enhancing stress dissipation and reducing localised deformation. Interstitial gaps between the strips were carefully filled with additional plywood segments to maintain the intended curvature and produce a continuous, seamless surface for veneer lamination.

Upon completion of this strip-planked substructure, 1 mm thick veneer sheets were manually laminated over the framework. Veneer was selected for its superior flexibility, which allows it to conform precisely to the underlying contours, and for its ability to produce a smooth, continuous surface suitable for further finishing. Each veneer sheet was bonded using adhesive and temporarily secured with staples to ensure uniform adhesion and accurate alignment with the curvature defined by the supporting structure.

The cold moulding process resulted in a smooth external hull surface, essential for minimizing hydrodynamic drag. Moreover, due to its simplicity, this technique proved to be cost-effective and procedurally efficient compared to advanced composite fabrication methods. Significantly, it allowed the student-led team valuable hands-on experience in composite hull construction, reinforcing practical understanding of fundamental fabrication principles.

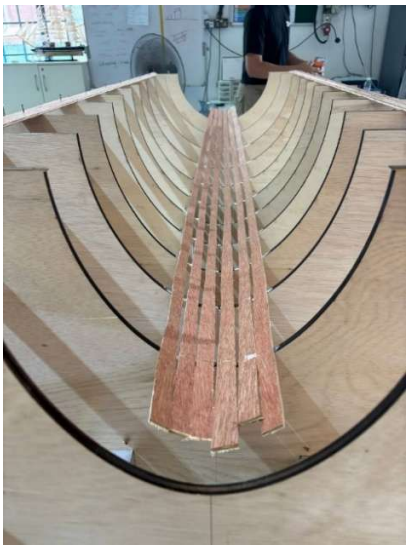

Figure 57: Skeletal Mould of the Submarine

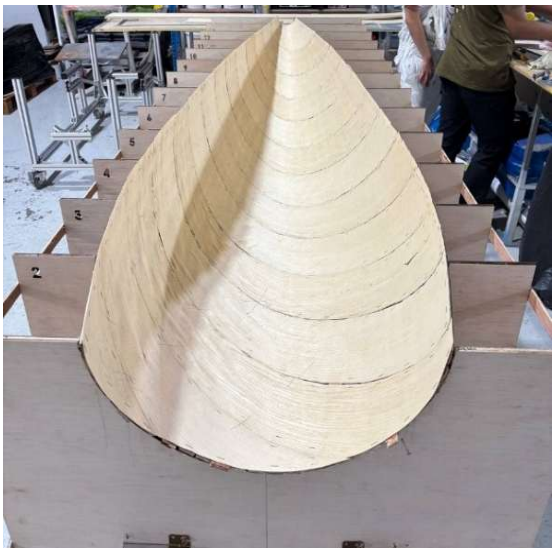

Figure 58: Veneers to form the Mould of the Submarine

The lamination process was executed in three successive repetitions, each involving the application of a 1 mm thick veneer layer. This staged approach served to progressively enhance surface smoothness, correct minor surface inconsistencies, and incrementally improve the structural stiffness of the mould, all while preserving the intended curvature of the hull. The cumulative effect of these three veneer layers was the formation of a smoother and more geometrically consistent surface, providing an optimal surface for subsequent fairing and composite layup. As this was the team's first attempt at constructing a negative mould, several surface irregularities were observed during the lamination phase. To address these imperfections and reinforce the mould surface, a single layer of chopped strand mat (CSM) fiberglass was laminated over the veneered structure CSM was selected due to its high conformability and ability to provide uniform reinforcement, attributes particularly beneficial when accommodating complex curves and varying surface textures commonly found in marine mould construction (Gurit, 2020).

Figure 59: Single Layer of Chopped Fiberglass

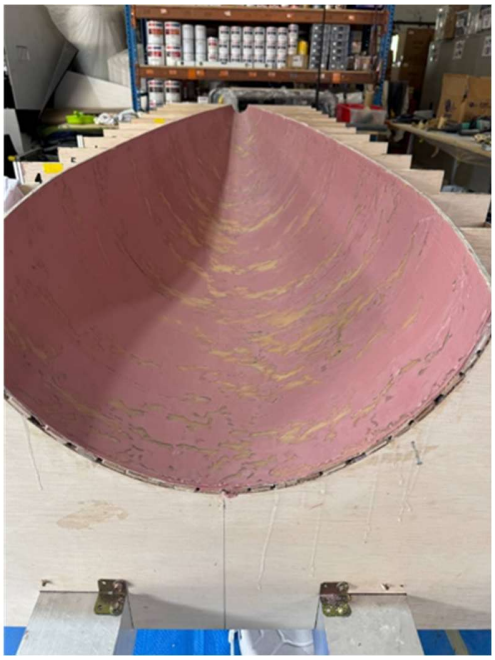

Figure 60: Fairing Compound Applied

Following the fiberglass application, surface refinement was conducted through a two-stage conditioning process. High spots on the surface were sanded to achieve a uniform contour and eliminate surface discontinuities, while low spots were filled using Awlfair (Shown in Figure: 61), a marine-grade epoxy-based fairing compound valued for its excellent workability, strong adhesion, and low shrinkage. This procedure ensured the formation of a smooth and continuous surface, suitable for final mould release treatment and subsequent composite fabrication.

This integrated approach, combining cold-moulded veneer lamination, fiberglass reinforcement, and precision fairing—exemplifies a hybrid construction methodology that optimally balances structural integrity, geometric fidelity, and fabrication practicality. It is particularly well-suited to educational and prototyping contexts, where iterative refinement and hands-on engagement constitute essential components of the learning process.

Figure 61: Final Painted Mould

The final stage of mould preparation involved the application of a gloss black paint across the entire surface, serving multiple functional purposes essential to the integrity of the composite fabrication process. Primarily, the paint created a non-porous, sealed barrier that enhanced the mould's resistance to moisture ingress and improved its overall durability, thereby contributing to the preservation of

dimensional stability throughout production. Additionally, the high-gloss finish reduced surface adhesion, facilitating a cleaner and less destructive demoulding process. The reflective properties of the black coating also supported quality assurance efforts by enabling the identification of inconsistencies in the subsequent application of release wax through variations in surface gloss and texture. (shown in Figure 62) This ensured comprehensive and uniform surface conditioning, thereby mitigating the risk of bonding defects during the lamination stage. Upon completion of this painting process, the mould was considered adequately conditioned for the application of release wax, marking the formal transition to the fiberglass layup phase under controlled fabrication conditions.

Figure 62: Applying of Wax

6.4 Hull fabrication

6.4.1 Fiberglass Lamination Process

Mako II was designed such that the top and bottom hulls are identical. This amounted to significant cost savings and the streamlining of the fabrication process.

To bond the composite layers, a two-part epoxy was used, consisting of Epicote 1006 Resin and Epicote 1006 Hardener. The components were mixed at a volume ratio of 1000 parts resin to 760 parts hardeners. This formulation was chosen for its compatibility with both the QA-1050 composite layers and the 3mm PET100 foam core in between, which helps ensure the effective fusion of the laminate structure, thereby providing structural integrity to the hull. Epoxy resin also provided superior bonding strength, enhanced durability, and excellent weight-to-strength ratio—key attributes for a high-performance human-powered submarine.

Figure 63: Mixing the Resin and Hardener

Figure 64: Layering the Fiberglass Sheets

Figure 65: Applying of Resin-Hardner Mixture onto the Fiberglass sheets

To further improve modularity, an aft cone was cut out, as shown in Figure 66.

Figure 66: Aft Cone Cut

Creating of hull joints

With the hull modular design consideration, L-brackets as the preferred connection between the top and bottom hull segments. These L-brackets are laminated with threaded aluminium plates to allow smooth assembly.

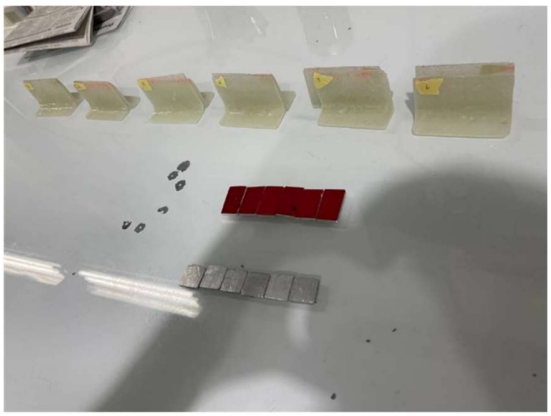

Figure 67 and 68: L Brackets and Metal Plates

6.4.2 Creating mounting points for the drivetrain

Reinforced mounting points were designed to anchor the drivetrain in place securely. These points were strategically positioned to ensure optimal force distribution.

Figure 69: Mounting Point for the Drivetrain

6.4.3Drilling of drain holes

To allow water to flow in and out efficiently, referencing rule 6.6.2, the submarine has four 50 mm drain holes, providing a total flow rate of about 0.0306 m^3/s. This allows the 0.49 m^3 volume to drain in just 16 seconds, well within the 3-minute guideline. Additionally, the gap between the propeller and the aft cone, along with the gap between the two hulls, also functions as a drainage path.

Figure 70: Drain Holes on the Bottom Hull

6.4.4 Hatches

Three hatches were integrated into the submarine: the pilot hatch (also known as the front hatch), the safety buoy hatch, and the maintenance hatch. The perimeters were carefully marked according to the measurements. The maintenance hatch was strategically placed near the stern to provide access to the bevel gears, control fin linkages, and access to the safety system. The safety hatch was designed as an open slot, allowing the buoy to exit freely when the dead man's switch is triggered. This ensures there is no interference during deployment.

Figure 71 and 72: Measurement, Labelling, and Cutting of the Hatches

Initially, ball latches were used to secure the hatches but aligning them proved difficult due to the internal curvature. Despite integrating them onto protrusions to reduce shear and aid alignment, the closure remained weak and inconsistent.

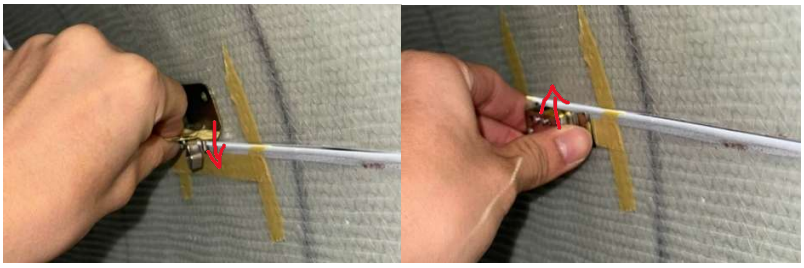

Figure 73 and 74: Top and Bottom Ball Latch initially used for Pilot Hatch

With the ball hatch assembly, Neodymium Grade N35 magnets with a durable, waterproof plastic coating and axial magnetization (through the thickness) were used to ensure the hatch remains securely closed. The plastic coating protects the magnets from water and physical damage, making them suitable for repeated use in demanding conditions. These magnets provide an approximate pull force of 15–20 kg, which is sufficient to keep the hatch closed while still allowing the pilot to egress quickly in an emergency.

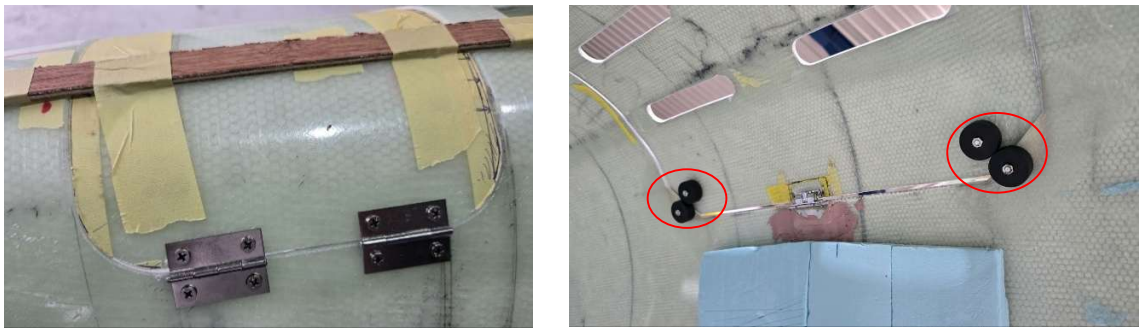

Figure 75 and 76: New Hinges and Magnets used for Pilot Hatch

6.5 Attaching the canopy

The canopy was installed at the front of the submarine, with small holes added at the top to let out the pilot's exhaled air. These vents prevent the entrapment of air, which would negatively impact the submarine's buoyancy.

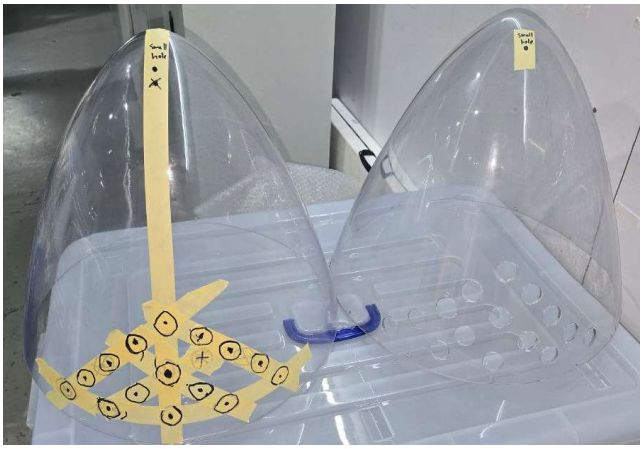

Figure 77: Holes for Canopy

6.6 Strobe light mountings

To comply with rule 6.5.5, custom 3D-printed housings were created to hold the strobe lights. Holes were carefully cut into the submarine's hull to accommodate the housings, ensuring a secure and precise fit for proper installation and visibility after attaching the lights onto the hull.

Figure 78 and 79: Strobe Light 3D Printed Mounting and Holes

7. Environmental Impact

As part of our commitment to sustainability, we adopted several environmentally friendly strategies in the design and construction of our second-edition human-powered submarine, MAKO II. One key approach was the reuse of components from our previous submarine, MAKO I. This not only aligns with environmentally responsible engineering practices but also highlights our team's resourcefulness and long-term planning.

A significant aspect of this reuse strategy was the decision to retain and repurpose the drivetrain system from MAKO I. As a mechanically complex and resource-intensive component, the drivetrain typically requires the fabrication of specialized parts. By reusing the existing system, we substantially reduced the need for new manufacturing, thereby minimizing the project's material waste. Furthermore, the proven performance of the original drivetrain enabled us to streamline the testing process and lessen our reliance on additional raw materials.

An additional design choice was making the hull symmetrical along the horizontal axis. This symmetry meant that only one half of the mould needed to be produced, as it could be used for both the fabrication of the top and bottom halves of the submarine. By doing so, we significantly reduced the amount of material and resources required for mould fabrication by cutting down on both waste and production costs. This efficient approach not only simplified the manufacturing process but also helped reduce material wastage.

Lastly, by reusing leftover buoyancy foam from MAKO I. After evaluating its condition and confirming its suitability, we incorporated the foam into MAKO II. This choice helped prevent unnecessary material waste and avoided the environmental and financial costs associated with sourcing and manufacturing new materials. By making deliberate choices to reuse durable components, we help reduce

the overall environmental impact of our project. While human-powered submarines already promote sustainable propulsion by relying solely on human energy, we sought to advance this principle further by embedding sustainability into every stage of our design and construction process.

8. General Arrangement

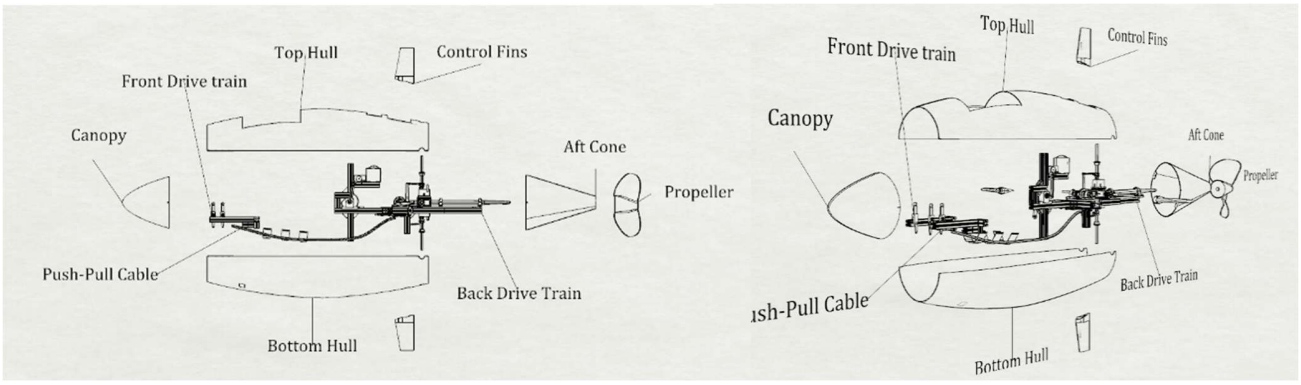

Figure 80: Drawing of the General Arrangement

9. Future Development & Lessons Learned

Future Development and Lessons Learned

The design and fabrication process of this year's submarine revealed several areas requiring improvement, which inform future development strategies.

Fabrication

Errors in technical drawings led to misalignments during assembly. Notably, the drivetrain had to be positioned 7 cm forward of its intended location, and the aft cone required an additional 5 cm to be trimmed. These issues highlight the need for more rigorous design validation and dimensional checks prior to fabrication.

Electrical System Reliability

The current electrical system demonstrates insufficient waterproofing, posing a risk to operational safety and long-term reliability. Enhancing waterproofing measures is critical for ensuring consistent electrical performance under submerged conditions.

Safety System Enhancements

The safety mechanisms require further refinement to ensure the pilot's protection during both normal operations and emergency scenarios. Improvements should focus on system responsiveness and ease of activation under stress.

Pilot Ergonomics and Internal Layout

The pilot's comfort and operational efficiency were limited by suboptimal control system positioning and restricted internal space. These constraints were exacerbated when the pilot wore a wetsuit, indicating a need to revisit the cockpit layout with a focus on ergonomic principles and mobility.

Buoyancy and Structural Issues

Several buoyancy-related issues were observed. The hull was not fully covered with Soric foam, leading to uneven buoyancy distribution. Additionally, inconsistencies in hull thickness were noted, and the hand lay-up fabrication method resulted in resin saturation problems. These issues compromised structural uniformity and affected overall buoyancy.

<u>Proposed Future Improvements</u>

To address the challenges, several development directions are recommended:

- Transition from hand lay-up to vacuum infusion to improve laminate quality and achieve uniform hull thickness.
- Further develop the pneumatic safety system to enhance reliability and operational readiness.
- Redesign the hatch mechanism to improve sealing, accessibility, and ease of use.

- Account for the varying weight of the air tank, which decreases over time and impacts the submarine's trim. This is particularly important given the reduced weight of this year's design, which increases sensitivity to weight distribution.
- Investigate and mitigate residual torque effects, which are more pronounced due to the lighter mass and reduced inertia of the current submarine model.

10. Summary/Conclusions

The design of the SIT Nautical Knights' second-generation human-powered submarine, MAKO II, represents a significant advancement in the team's engineering philosophy, which centres on achieving high performance, operational safety and modular construction. Building upon the insights gained from previous year's European International Submarine Race, the team redefined its design objectives for the 2025 International Submarine Races to focus on a straight-line, high-speed performance through the team's refined and systematic design process.

A structured methodology guided the project development, encompassing 3D modelling of each system's prototype, computational fluid dynamics (CFD) simulations and material evaluation. More than 50 hull configurations were analysed, with the final design demonstrating a 15% reduction in drag relative to the previous iteration. This outcome was achieved through the adoption of a lighter, modular hull constructed using QUADRIAXIAL QA-1050 fibreglass and a PET100 foam core, alongside a redesigned drivetrain and a two-bladed Wageningen B-series propeller optimised for operation at 300 revolutions per minute

The control surface configuration was reengineered using a NACA 0018 aerofoil, scaled down to 80% of its previous dimensions, and was selected over the NACA 0012 due to its superior post-stall behaviour and greater stability in turbulent flow conditions. The drivetrain system was modularised and equipped with cleat pedals and corrosion-resistant materials, thereby enhancing both mechanical reliability and ease of maintenance.

Safety was prioritised through the development and testing of a mechanical dead man's switch, reinforced pilot escape procedures, and a deployable buoy system compliant with ISR safety protocols. Comprehensive testing was conducted at Singapore Polytechnic and the Republic of Singapore Navy's Naval Diving Unit pool, during which the submarine accumulated 52 hours of underwater trials. These tests verified the structural integrity, hydrodynamic performance, emergency preparedness, and pilot control systems of the submarine.

The MAKO II project not only achieved its technical performance objectives but also exemplified the value of interdisciplinary collaboration and experiential learning. Through a rigorous and iterative design process, the SIT Nautical Knights successfully developed a high-performance, human-powered submarine capable of representing Singapore as the first Southeast Asian team at the 18th International Submarine Race. The project highlights the team's commitment to innovation, engineering excellence, and regional leadership in maritime technology.

11. Bibliography

[1] V. Kaushik, A. Wandile, V. Girade, and C. Khadse, “2D Simulation to Study the Effect of Flaps on Various Aerofoils at Different Angles,” in Recent Advances in Mechanical Infrastructure, A. K. Parwani, P. Ramkumar, K. Abhishek, and S. K. Yadav, Eds., Lecture Notes in Intelligent Transportation and Infrastructure, Springer, Singapore, 2022. Available at: https://doi.org/10.1007/978-981-16-7660-4_24

[2] Carlton, J. (2018), “Marine Propellers and Propulsion (Second Edition)”. Butterworth-Heinemann. Available at: https://pdfcoffee.com/marine-propellers-and-propulsion-second-editionjs-carlton2007-pdf-free.html

[3] Easy Composites (2021). 3Dcore PET 100 infusion foam. 3DCore Honeycomb Foam for Infusion; 3mm, 5mm, 10mm - Easy Composites. Available at: https://www.easycomposites.eu/3d-core-infusion-foam-core

[4] Epoxy archives. Wee Tee Tong. Available at: https://www.weeteetong.com/product-categories/epoxy/

[5] Gurit. (2020). Composite Materials and Engineering Solutions for the Marine Industry. Gurit Holding AG. Retrieved from https://www.gurit.com

[6] Khan, Sher. (2018). CFD analysis of human powered submarine to minimize drag. International Journal of Mechanical and Production Engineering Research and Development. 8. 10.24247/ijmperdjun2018111.

Appendices

Appendix 1: Hull selection matrix

Criteria	Weight	Hull #G	
		Rating	Weighted Score
Sufficient space for pilot and pedalling	4	5	20
Sufficient space for Drivetrain and modifications	3	3	9
Drag reduction %	3	4	12
Internal Volume	2	3	6
Surface Area	1	2	2
Total			49

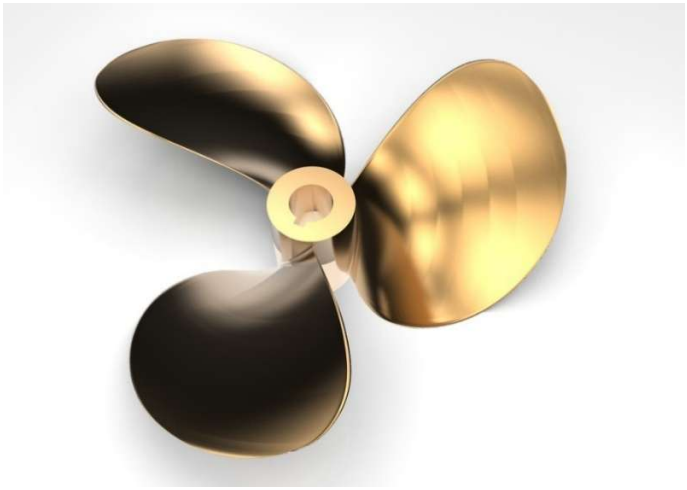

Appendix 2: Wageningen B-Series Propeller